NATIONAL ADVISORY COMMITTEE FOR AERONAUTICS

TECHNICAL NOTE 4173

AN ANALYTICAL INVESTIGATION OF THE GUST-ALLEVIATING PROPERTIES OF A SIMPLE PITCH DAMPER

By Norman L. Crabill

Langley Aeronautical Laboratory
Langley Field, Va.

Washington
December 1957

NATIONAL ADVISORY COMMITTEE FOR AERONAUTICS

TECHNICAL NOTE 4173

AN ANALYTICAL INVESTIGATION OF THE GUST-ALLEVIATING PROPERTIES OF A SIMPLE PITCH DAMPER

By Norman L. Crabill

SUMMARY

The response to atmospheric gusts of a lightly damped airplane model flying at a Mach number of 0.7 at sea level has been studied analytically with elevator fixed and with varying amounts of viscous restraint of a mass-overbalanced elevator. Although in a sharp-edge gust the viscously restrained mass-overbalanced elevator has negligible effect on the motion of the airplane center of gravity until the first peak in the normal-acceleration response of the model has been reached, the effective damping ratio of the subsequent motion can be more than trebled by a suitable choice of viscous restraint with some reduction in frequency of oscillation. In continuous gusts, calculations indicate that for the model considered there results a 20-percent reduction in root-mean-square normal acceleration at the center of gravity over a broad range of elevator viscous restraint.

INTRODUCTION

Aircraft operating in gusty air experience loads which can be divided into two types, according to their source: (1) loads due to the direct effect of the gust and (2) loads due to motions induced by the direct gust loads. Loads of the first type increase with airspeed and air density (see ref. 1), and those of the second type are significantly dependent on the damping ratio of the short-period oscillation of the airplane (see ref. 2) and the airplane relative-density factor (see ref. 1).

With lightly loaded well-damped airplanes, the motions induced by the gusts serve to reduce considerably the overall loads in rough air; however, with heavily loaded lightly damped airplanes, the reduction due to the motions is much less. Thus, means of gust-loads reduction become increasingly more desirable as the airplane relative-density factor increases and the short-period damping decreases. This reduction can be achieved (1) by countering the direct effect of the gust (see, for example, refs. 1 and 3 to 10) and (2) for airplanes with low damping ratios,

by altering the motions induced by the direct gust loads by increasing the short-period damping ratio. To date there has been relatively little work in this second direction, perhaps because of the limited alleviation that might be expected from such a system (see ref. 11).

The purpose of the present paper is to investigate analytically the alleviation that can be obtained by a relatively simple system which alters the longitudinal motions induced by the direct effect of the gust loads. This simple system consists of a mass-overbalanced viscously restrained elevator and is analogous to the simplified yaw damper reported in reference 12. The calculations presented in this paper are limited to an airplane model flying at one altitude and at one speed. This airplane model has a relatively large pitching radius of gyration and static margin. Calculations were made for a wide range of viscous restraint, and the resulting reductions in normal acceleration at the center of gravity were determined.

ANALYSIS

Description of System and Outline of Analysis

The system studied in this paper is an airplane with a mass-overbalanced viscously restrained elevator and is similar to the simplified yaw-damper system reported in reference 12, except for the use of mass overbalance in lieu of adjusted hinge-moment parameters. It was decided to use elevator mass overbalance in this investigation because of its inherent simplicity and the difficulty in predicting the effect of elevator modifications on hinge moment. The system has seven degrees of freedom for the rigid airplane, but when the motions are restricted to the longitudinal modes with essentially constant forward speed, only three degrees of freedom remain: vertical translation of the center of gravity of the airplane, rotation of the airplane about the lateral axis through the center of gravity, and rotation of the elevator about its hinge axis. In the following analysis, the differential equations governing the motions of this system in its three degrees of freedom are set up, and the dynamic stability of the system is studied from the roots of the characteristic equation. Then, the response of the system to a unit step gust input (indicial response function) is obtained and used to obtain the response to continuous sinusoidal turbulence (the frequency-response function). Finally, the root-mean-square normal acceleration in continuous random turbulence is obtained by utilizing power-spectral-density techniques.

Equations of Motion

In the analysis the usual assumptions pertinent to the longitudinal dynamic stability of a rigid aircraft with free elevators were made. The resulting differential equations of motion, based on the body-axis system shown in figure 1, are

$$F_Z = mV(\dot{\alpha} - \dot{\theta}) = qS\left(C_{Z_\alpha}\alpha + C_{Z_\delta}\delta\right) \tag{1}$$

$$M_Y = I_Y\ddot{\theta} = qS\bar{c}\left(C_{m_\alpha}\alpha + \frac{\bar{c}}{V}C_{m_{\alpha'}}\dot{\alpha} + \frac{\bar{c}}{V}C_{m_{\theta'}}\dot{\theta} + C_{m_\delta}\delta + \frac{\bar{c}}{V}C_{m_{\delta'}}\dot{\delta}\right) \tag{2}$$

$$M_h = I_e(\ddot{\theta} + \ddot{\delta}) + l_e m_e x_e\ddot{\theta} - m_e x_e V(\dot{\theta} - \dot{\alpha})$$

$$= qS_e\bar{c}_e\left(C_{h_\alpha}\alpha + \frac{\bar{c}_e}{V}C_{h_{\alpha'}}\dot{\alpha} + \frac{\bar{c}_e}{V}C_{h_{\theta'}}\dot{\theta} + C_{h_\delta}\delta + \frac{\bar{c}_e}{V}C_{h_{\delta'}}\dot{\delta}\right) \tag{3}$$

(The symbols are defined in appendix A.) The force F_Z is related to a_n through the equation

$$a_n = -\frac{F_Z}{W} \tag{4}$$

The characteristic equation obtained from these differential equations is given in appendix B and has the form

$$\lambda\left(A\lambda^4 + B\lambda^3 + C\lambda^2 + D\lambda + E\right) = 0 \tag{5}$$

The characteristic equation (5) is of fifth degree with one zero root, and there are three distinct types of motions, depending on the value of $C_{h_{\delta'}}$. If the value of $C_{h_{\delta'}}$ is less than a certain critical value, there result two sets of complex conjugate roots corresponding to the oscillatory airframe and elevator modes and the one zero root which represents the indifference of the airplane to pitch attitude. If $C_{h_{\delta'}}$ exceeds the critical value, two unequal negative real roots result, representing the exponential decay of the elevator mode; the airframe mode is still represented by the complex conjugate pair and the zero root. If $C_{h_{\delta'}}$ equals the critical value, the two negative

roots are equal. This condition corresponds to critical damping of the elevator mode. This special case is not dealt with in this paper.

Response to Unit Step Gust Input

An elaborate formulation of the problem of the response of the system to a unit step gust input, such as that given by Mazelsky and Diederich (ref. 13) and Brenner and Isakson (ref. 14) is not given herein. Instead, the normal-acceleration indicial-response model proposed by Press and Mazelsky (ref. 2) was used in a modified form. In this normal-acceleration response model it is assumed that after the airplane encounters a step gust directed normal to the flight path "the shape of the response curve up to the peak acceleration depends primarily on the gust penetration function (Küssner function). After the peak value . . . the character of the response appears to be primarily a function of airplane stability and to approximate the short-period oscillation of the airplane." (See ref. 2.) Or, in equation form,

$$a_n(s) = a_{n,max} \sin \frac{\pi}{2} \frac{s}{s_p} \qquad (0 < s < s_p) \qquad (6)$$

$$a_n(s) = a_{n,max} e^{\alpha_1 (s - s_p)} \cos \beta (s - s_p) \qquad (s_p < s) \qquad (7)$$

This response model has been used successfully by Vitale, Press, and Shufflebarger (ref. 15) in predicting root-mean-square normal acceleration on a transonic tailless rocket-propelled model. In the present study a more nearly exact representation of the short-period oscillation was used and the penetration effect on the tail was accounted for in an approximate manner that agrees at least qualitatively with the tail effects shown by Mazelsky and Diederich (ref. 13) and Brenner and Isakson (ref. 14). In reference 14, it is seen that the tail begins to develop an appreciable fraction of its quasi-steady lift only after it penetrates several tail chords into the gust and that, for high mass ratios, practically no translation or pitching occurs until this time. Accordingly, it was assumed that

(1) No vertical translation or pitching of the airplane occurred until after the tail had penetrated 2 tail chords into the gust (total penetration of 4 wing chords).

(2) The wing lift equaled its quasi-steady value after it had penetrated 4 wing chords into the gust and was a sine function of the penetration distance before this time.

(3) The tail lift equaled its quasi-steady value after it had penetrated 2 tail chords into the gust and was zero before this time.

The assumptions are not valid for all airplanes, but are thought to apply sufficiently well for this configuration in a heavily loaded condition (high mass ratio). The discontinuous development of the tail lift causes discontinuities in normal acceleration and pitching moment which approximate the more exact variations indicated by reference 14 for an airplane with a high mass ratio.

The elevator effects were treated by assuming that

(1) The transient aerodynamic hinge moments occurring up to the first peak were insignificant in comparison with the artificial viscous hinge moments and the inertia moments of the mass-overbalanced elevator.

(2) Subsequent to the first peak, the aerodynamic hinge moments could be represented adequately by quasi-steady values.

The normal-acceleration and pitching responses up to 4 wing chords penetration can be written down immediately as a consequence of the assumptions. Thus, since $\alpha_g = \frac{1}{V}$,

$$a_n = -\frac{F_Z}{W} = \left(\frac{-C_{Z_\alpha,WB}}{m_1}\frac{1}{g}\right)\sin\frac{\pi}{2}\frac{t}{t_p} \tag{8}$$

$$\theta = 0 \tag{9}$$

The elevator motion obtained by solving equations (1) and (3) simultaneously subject to the conditions of equations (8) and (9) and of zero aerodynamic hinge moment but with artificial viscous restraint is given by

$$\delta = K_2\left[\frac{-1}{\omega_o K_1} + \left(\frac{1}{\omega_o^2 + K_1^2}\right)\left(\frac{\omega_o}{K_1}e^{K_1 t} - \sin\omega_o t + \frac{K_1}{\omega_o}\cos\omega_o t\right)\right] \tag{10}$$

As was pointed out previously, it is assumed that, subsequent to the first acceleration peak, the airplane is free of unsteady-lift effects due to penetration into the gust; that is, its lift can be given adequately by quasi-steady values. This assumption is equivalent to the assumption that the model responds essentially in its short-period longitudinal motion subject to the initial conditions

$$\left.\begin{aligned} \alpha(t_p) &= \frac{1}{V} \\ \theta(t_p) &= 0 \\ \delta(t_p) &= \delta_p \\ \dot{\theta}(t_p) &= 0 \\ \dot{\delta}(t_p) &= \dot{\delta}_p \end{aligned}\right\} \tag{11}$$

where δ_p and $\dot{\delta}_p$ are obtained from equation (10) at $t = t_p$. The solutions of equations (1), (2), and (3) subject to the initial conditions given by equations (11) are the solutions required. These solutions, representing a_n for the two types of motions, are given as functions of the nondimensional penetration distance $s = \frac{Vt}{\bar{c}}$:

For $C_{h_{\delta'}} < \left(C_{h_{\delta'}}\right)_{cr}$,

$$a_n(s) = \left(\frac{-C_{Z_\alpha}}{m'}\frac{V}{g}\right)\left\{e^{\alpha_1(s-s_p)}\left[A_1 \cos\beta(s - s_p) + B_1 \sin\beta(s - s_p)\right] + e^{\alpha_2(s-s_p)}\left[C_1 \cos\Delta(s - s_p) + D_1 \sin\Delta(s - s_p)\right]\right\} \tag{12}$$

For $C_{h_{\delta'}} > \left(C_{h_{\delta'}}\right)_{cr}$,

$$a_n(s) = \left(\frac{-C_{Z_\alpha}}{m'}\frac{V}{g}\right)\left\{e^{\alpha_1(s-s_p)}\left[A_1 \cos\beta(s - s_p) + B_1 \sin\beta(s - s_p)\right] + C_1 e^{\alpha_3(s-s_p)} + D_1 e^{\alpha_4(s-s_p)}\right\} \tag{13}$$

For $C_{h_{\delta'}} = -\infty$ (elevator fixed),

$$a_n(s) = \left(\frac{-C_{Z_\alpha}}{m'}\frac{V}{g}\right)\left\{e^{\alpha_1(s-s_p)}\left[A_1 \cos\beta(s - s_p) + B_1 \sin\beta(s - s_p)\right]\right\} \tag{14}$$

The expressions for θ and δ are similar and are given in appendix C together with the procedure for the determination of the constants A_1, B_1, C_1, and D_1.

Note that, for the elevator-fixed case, the representation of the short-period mode (eq. (14)) contains a sine term which does not appear in the simplified representation assumed by Press and Mazelsky (eq. (7)). Although the resulting representation of the short-period mode (eq. (14)), is more nearly exact, it is only an approximate representation of the oscillatory response of the airplane subsequent to the first peak, since the penetration effects on the aerodynamic derivatives probably persist for more than the 4 chords assumed.

Response to Continuous Gusts

The gust frequency-response function or the response of the airplane to an infinitely long succession of gusts of the form

$$\alpha_g = \frac{1}{V} \sin \omega_g t \tag{15}$$

can be obtained from the normal-acceleration indicial-response functions (eqs. (12) and (13)) by the relation

$$F_n(i\nu) = i\nu \int_0^\infty a_n(s) e^{-i\nu s} ds \tag{16}$$

where $\nu = \frac{\omega_g \bar{c}}{V}$. The integrations for the two cases have been performed and are given in appendix D. For subsequent calculations with the atmospheric power-spectral-density function, the frequency variable $\nu = \frac{\omega_g \bar{c}}{V}$ is transformed to $\Omega = \frac{\omega_g}{V}$. Thus Ω is independent of the airplane speed and size and is based solely on atmospheric characteristics.

The power spectrum of the normal acceleration was computed from the equation

$$\Phi_n(\Omega) = \Phi_{atmos}(\Omega) \left| F_n(i\Omega) \right|^2 \tag{17}$$

The power-spectral-density function of the atmosphere was assumed to be given by

$$\Phi_{atmos}(\Omega) = \frac{(\text{Intensity constant})^2}{\Omega^2} = \frac{1}{\Omega^2} \tag{18}$$

In the present study, variations in atmospheric gust intensity were not considered and the unit intensity constant was used for all calculations.

The root-mean-square normal acceleration was then found from the relation

$$\sigma_n = \left[\int_0^\infty \Phi_n(\Omega)d\Omega\right]^{1/2} \tag{19}$$

These results (eqs. (17) to (19)) from the generalized harmonic analysis of gust loads are taken from reference 2.

CALCULATIONS AND RESULTS

An outline drawing of the airplane configuration chosen for application of the foregoing theory is given in figure 2. The straight horizontal tail was chosen to give a straight hinge line. Some of the pertinent characteristics of this airplane are given in table I. The size was chosen to be comparable to the rocket-powered models tested by Vitale, Press, and Shufflebarger (ref. 15). The aerodynamic characteristics of the wing-body combination were based on tests by Spreemann and Alford (ref. 16); the tail and elevator data were taken from results of a test by Turner (ref. 17).

When this investigation was first undertaken, the roots of the characteristic equation were obtained for this airplane with a mass-balanced elevator; the results indicated relatively little effect of the elevator mode on the airframe mode for any value of $C_{h_{\delta'}}$. A value of mass overbalance (x_e negative) sufficient to halve the E term in the characteristic equation was chosen for further calculations. For lg flight under the assumed flight conditions, the trim elevator angle corresponding to the mass overbalance was -0.47°.

The period and damping of both the airframe and the elevator short-period modes are given in figure 3 as functions of $C_{h_{\delta'}}$. (Note that $C_{h_{\delta'}} = -\infty$ corresponds to elevator fixed.) The gust indicial responses in a_n and δ are shown in figure 4 for $C_{h_{\delta'}} = 0, -62.5, -175$, and $-\infty$; the θ, $\dot{\theta}$, and $\dot{\delta}$ responses are also given for $C_{h_{\delta'}} = -175$ and $-\infty$. The remaining calculations were done for $C_{h_{\delta'}} = 0, -62.5, -175, -250$, and $-\infty$.

The amplitude ratios of the normal-acceleration gust-frequency-response functions and the corresponding power-spectral-density functions are shown in figures 5 and 6, respectively. The root-mean-square normal-acceleration response (fig. 7) was then determined by graphically integrating $\Phi_n(\Omega)$.

DISCUSSION

Stick-Free Stability

The effect of viscous elevator restraint on the classical stick-free stability of the airplane is shown in figure 3. It is seen that the addition of viscous damping can more than treble the effective damping of the airplane short-period mode (as compared with stick-fixed), and is extremely effective in improving the damping of the elevator mode as could be expected. (Note that $C_{h_{\delta'}}$ due to aerodynamic effects alone is only on the order of -1 to -10.) In the vicinity of $C_{h_{\delta'}} = -80$, the aforementioned critical value of $C_{h_{\delta'}}$ is reached. At this point the oscillatory elevator mode disappears and is replaced by two exponential convergences; for further increases in $C_{h_{\delta'}}$ the motion can be practically represented by a single exponential decay. It is interesting to observe that the peak in the airframe-period curve occurs in the vicinity of $(C_{h_{\delta'}})_{cr}$.

Gust Response

Discrete gusts.- Comparison of the time histories of the gust indicial responses for $C_{h_{\delta'}} = 0, -62.5, -175$, and $-\infty$ (fig. 4) shows that viscously restraining the elevator markedly influences the motion subsequent to the first peak. For $C_{h_{\delta'}} = -175$, $\zeta_a = 0.565$, and the subsequent oscillations practically disappear in one cycle; whereas for $C_{h_{\delta'}} = -\infty$, $\zeta_a = 0.175$, and about one-third of the original amplitude remains after 1 cycle. This favorable effect of the elevator motion is accomplished with only small elevator deflections ($\delta = 0.05^\circ$) and velocities ($\dot{\delta} = 2.2^\circ$ per second) for a gust velocity of 1 foot per second. Hence the drag penalty due to the action of the elevators would be insignificant.

Continuous gusts.- The normal-acceleration gust-frequency-response function for $C_{h_{\delta'}} = 0$ (fig. 5(a)) exhibits two peaks; the low-frequency peak corresponds to the oscillatory airframe mode and the higher frequency peak to the oscillatory elevator mode. In considering the magnitude of the elevator-mode peak, it must be kept in mind that there is no damping at all in the elevator circuit, and the addition of even a slight amount

of viscous restraint corresponding to the aerodynamic damping of the elevator ($C_{h_{\delta'}} = -1$ to -10) would substantially lower this peak (see fig. 3(b)). The small amount of damping which exists in the elevator mode is provided by the dynamic coupling with the airframe mode. For $C_{h_{\delta'}} = -62.5$, although the elevator motion is still oscillatory, the peak has disappeared. For values of $\nu > 0.2$, the frequency-response function is practically the same for all values of $C_{h_{\delta'}}$ because of the predominating contribution of the initial quarter sine wave in the normal-acceleration indicial response at these frequencies.

The power spectrum of the normal-acceleration response (fig. 6) indicates that practically all the power in the normal-acceleration response occurs near the natural frequency of the airframe. Note that, for $C_{h_{\delta'}} = -175$, the normal acceleration at the airframe natural frequency has been reduced 48 percent below that experienced with $C_{h_{\delta'}} = -\infty$ but that at lower frequencies the acceleration is somewhat greater.

The principal results of this investigation are presented in figure 7. Therein, the root-mean-square normal acceleration of the airplane in continuous rough air, normalized with respect to that obtained with fixed elevator, is given for four values of viscous restraint. The ratio $\sigma_n/\sigma_{n,\delta \text{ fixed}}$ is seen to be about 1.07 for no viscous restraint and decreases rapidly with the initial increase in $C_{h_{\delta'}}$. A flat minimum of about 20-percent alleviation is reached for $C_{h_{\delta'}} = -125$ to -250; although computations were not made for higher values of $C_{h_{\delta'}}$, it seems reasonable to expect that the curve would follow a gradual upward trend with increasing $C_{h_{\delta'}}$ and approach 1.0 asymptotically.

The dashed line in figure 7 labeled "Simple indicial-response model" is based on the simplified response model used by Press and Mazelsky (eqs. (6) and (7)) and permits the determination of σ_n if the effective values of airplane short-period stability parameters, that is, damping ratio ζ_a and frequency b_a, be known. The omission of the airframe sine term from the indicial response model (see eqs. (12) to (14)) evidently causes the simplified method to overestimate the alleviation near optimum $C_{h_{\delta'}}$ and to underestimate it for low values.

Other considerations.- In all the foregoing analysis and application, the moments acting on the elevator have been assumed to be significantly larger than moments due to static friction. Also, no provision was made for elevator control, since the elevator used for the analysis occupied the entire exposed trailing edge of the tail. In a practical application to an actual airplane, it might be feasible to employ a split elevator,

one-half being used for control and one-half being used for auxiliary damping. Such an arrangement would also insure that the elevator motions required for damping would not be interfered with by the action of the pilot in holding the control stick. The system could be optimumized at cruising speeds; if the action of the system proved objectionable at the lower speeds experienced during climb and descent, it could be locked out, since the highest speeds likely to be attained are the critical speeds.

The effects of changes in speed, Mach number, and altitude on the optimum values of $C_{h_{\delta'}}$ have not been investigated and the optimum values of I_e, x_e, C_{h_α}, and C_{h_δ} for this and other values of static margin have not been determined. Also, since mass overbalance is used, there would be a small hinge moment due to longitudinal accelerations and a reduction in stability in steady pull-ups, with possibly some effect on the phugoid mode. In spite of these possible effects, the system does appear to offer a usable margin of gust-load alleviation for lightly damped aircraft, and it is especially attractive in view of its inherent simplicity and reliability.

CONCLUDING REMARKS

The gust response of a lightly damped airplane model flying at a Mach number of 0.7 at sea level has been studied analytically with elevator fixed and with varying amounts of viscous restraint of the mass-overbalanced elevator. Although the viscously restrained mass-overbalanced elevator probably has negligible effect on the airplane motion until the first peak in the normal-acceleration response to a sharp-edge gust has been reached, the effective damping ratio of the subsequent motion can be more than trebled by a suitable choice of viscous restraint with some reduction in frequency of oscillation. In continuous gusts, calculations indicate that for the model considered there results a 20-percent reduction in root-mean-square normal acceleration at the center of gravity over a broad range of elevator viscous restraint.

Langley Aeronautical Laboratory,
National Advisory Committee for Aeronautics,
Langley Field, Va., September 10, 1957.

APPENDIX A

SYMBOLS

Positive directions of displacements, velocities, and accelerations are shown in figure 1.

a real part of characteristic-equation root pertaining to airframe mode

a_n normal-acceleration increment from trim due to gust of 1 ft/sec, g units

b imaginary part of characteristic-equation root pertaining to airframe mode

c real part of characteristic-equation root pertaining to elevator root

$\bar{c}$ mean aerodynamic chord of total wing

$\bar{c}_e$ mean aerodynamic chord of exposed elevator

$$C_h = \frac{M_h}{qS_e\bar{c}_e}$$

$$C_m = \frac{M_Y}{qS\bar{c}}$$

$$C_Z = \frac{F_Z}{qS}$$

d imaginary part of characteristic-equation root pertaining to elevator mode

e base of natural logarithms, 2.7182 . . .

$F_n(i\nu), F_n(i\Omega)$ gust frequency-response functions

F_Z force parallel to Z-axis

g acceleration due to gravity, 32.17 ft/sec^2

$i = \sqrt{-1}$

$K_1 = \frac{C_{h_{\delta'}}}{I_{e,2}}$

$K_2 = -\frac{m_e x_e}{I_e} \frac{C_{Z_{\alpha,WB}}}{m_1}$

I_e mass moment of inertia of elevator about hinge axis

$I_{e,1} = \frac{I_e}{qS\bar{c}_e}$

$I_{e,2} = I_{e,1} \frac{V}{\bar{c}_e}$

I_Y mass moment of inertia of airplane about lateral axis through center of gravity

$I_{Y,1} = \frac{I_Y}{qS\bar{c}}$

$I_{Y,2} = I_{Y,1} \frac{V}{\bar{c}}$

l_e distance from center of gravity of model to center of gravity of elevator

m mass of airplane

$m_1 = \frac{mV}{qS}$

m_e mass of elevator

M_h aerodynamic hinge moment on elevator taken about hinge axis

M_Y pitching moment about center of gravity

M_∞ free-stream Mach number

P period of oscillatory motion, sec

q dynamic pressure, lb/sq ft

s distance penetrated into gust, taken from leading edge of exposed wing root chord, $\frac{Vt}{\bar{c}}$

S wing area

t time

$t_{1/2}$ time for motion to damp to one-half amplitude

u component of V along X-axis

V free-stream airspeed

W weight

w component of V along Z-axis

x_e distance from elevator hinge axis to center of gravity of elevator, positive when center of gravity is rearward of hinge axis

X longitudinal body axis, positive forward

Y lateral axis, positive toward right wing tip

Z normal body axis, positive downward

α angle of attack, radians

$\alpha_1 = \frac{a\bar{c}}{V}$

$\alpha_2 = \frac{c\bar{c}}{V}$

$\alpha_3 = \frac{\lambda_3\bar{c}}{V}$

$\alpha_4 = \frac{\lambda_4\bar{c}}{V}$

$\alpha_g = \frac{l}{V}$

$\beta = \frac{b\bar{c}}{V}$

γ flight-path angle, radians

δ elevator displacement, radians (unless otherwise noted)

$\Delta = \frac{d\bar{c}}{V}$

ζ damping ratio

θ pitch attitude, deg

$\nu = \frac{\omega_g \bar{c}}{V}$

σ_n root-mean-square normal acceleration

$\Phi_{atmos}(\Omega)$ power-spectral-density function of the atmosphere

$\Phi_n(\Omega)$ power-spectral-density function of the normal-acceleration response in continuous rough air

ω_g circular frequency of sinusoidal gusts

$\omega_s = \frac{\pi}{2s_p}$

$\omega_o = \frac{\pi}{2t_p}$

$\Omega = \frac{\omega_g}{V}$

Subscripts:

a airframe

cr critical

e elevator

WB wing-body

p pertaining to the first peak in the normal-acceleration response

δ_{fixed} elevator fixed

Derivatives are denoted by subscript notation, thusly:

$$C_{Z_\alpha} = \frac{\partial C_Z}{\partial \alpha} \quad \text{and so forth}$$

Differentiation with respect to time is denoted by a dot, thusly:

$$\dot{\alpha} = \frac{d\alpha}{dt}$$

whereas differentiation with respect to distances (in wing chord lengths) is denoted by a prime, thusly:

$$\alpha' = \frac{d\alpha}{ds} = \frac{\dot{\alpha}}{V/\bar{c}} = \frac{d\alpha}{dt}\frac{\bar{c}}{V}$$

however,

$$\delta' = \frac{d\delta}{dt}\frac{\bar{c}_e}{V}$$

APPENDIX B

THE CHARACTERISTIC EQUATION

The characteristic equation obtained from the equations of motion is

$$\lambda\left(A\lambda^4 + B\lambda^3 + C\lambda^2 + D\lambda + E\right) = 0 \tag{B1}$$

where

$$A = 1 \tag{B2}$$

$$B = \frac{-C_{h_{\delta'}}}{I_{e,2}} - \left(\frac{C_{m_{\theta'}}}{I_{Y,2}} + \frac{C_{m_{\alpha'}}}{I_{Y,2}} + \frac{C_{Z_\alpha}}{m_1}\right) + \left(1 + \frac{l_e m_e x_e}{I_e}\right)\frac{C_{m_{\delta'}}}{I_{Y,2}} \tag{B3}$$

$$C = \frac{C_{h_{\delta'}}}{I_{e,2}}\left(\frac{C_{m_{\theta'}}}{I_{Y,2}} + \frac{C_{m_{\alpha'}}}{I_{Y,2}} + \frac{C_{Z_\alpha}}{m_1}\right) - \frac{C_{m_\alpha}}{I_{Y,1}} + \left(1 + \frac{l_e m_e x_e}{I_e}\right)\frac{C_{m_\delta}}{I_{Y,1}} - \frac{C_{h_\delta}}{I_{e,1}} +$$

$$\frac{C_{Z_\alpha}}{m_1}\left[\frac{C_{m_{\theta'}}}{I_{Y,2}} - \left(1 + \frac{l_e m_e x_e}{I_e}\right)\frac{C_{m_{\delta'}}}{I_{Y,2}}\right] + \frac{C_{Z_\delta}}{m_1}\left[\left(1 + \frac{l_e m_e x_e}{I_e}\right)\frac{C_{m_{\alpha'}}}{I_{Y,2}} -$$

$$\left(\frac{C_{h_{\delta'}}}{I_{Y,2}} - \frac{V m_e x_e}{I_e}\right)\right] - \frac{C_{m_{\delta'}}}{I_{Y,2}}\left(\frac{C_{h_{\alpha'}}}{I_{e,2}} + \frac{C_{h_{\theta'}}}{I_{e,2}}\right) \tag{B4}$$

$$D = \frac{-C_{h_{\delta'}}}{I_{e,2}}\left(\frac{C_{m_{\theta'}}}{I_{Y,2}}\frac{C_{Z_\alpha}}{m_1} - \frac{C_{m_\alpha}}{I_{Y,1}}\right) + \frac{C_{Z_\alpha}}{m_1}\left[\frac{C_{h_\delta}}{I_{e,1}} + \left(\frac{C_{h_{\theta'}}}{I_{e,2}} + \frac{Vm_e x_e}{I_e}\right)\frac{C_{m_{\delta'}}}{I_{Y,2}} - \left(1 + \frac{l_e m_e x_e}{I_e}\right)\frac{C_{m_\delta}}{I_{Y,1}}\right] + \frac{C_{Z_\delta}}{m_1}\left[\left(1 + \frac{l_e m_e x_e}{I_e}\right)\frac{C_{m_\alpha}}{I_{Y,1}} - \frac{C_{h_\alpha}}{I_{e,1}} - \left(\frac{C_{h_{\theta'}}}{I_{e,2}} + \frac{Vm_e x_e}{I_e}\right)\frac{C_{m_{\alpha'}}}{I_{Y,2}} + \left(\frac{C_{h_{\alpha'}}}{I_{e,2}} - \frac{Vm_e x_e}{I_e}\right)\frac{C_{m_{\theta'}}}{I_{Y,2}}\right] + \frac{C_{h_\delta}}{I_{e,1}}\left(\frac{C_{m_{\theta'}}}{I_{Y,2}} + \frac{C_{m_{\alpha'}}}{I_{Y,2}}\right) - \frac{C_{m_\delta}}{I_{Y,1}}\left(\frac{C_{h_{\alpha'}}}{I_{e,2}} + \frac{C_{h_{\theta'}}}{I_{e,2}}\right) - \frac{C_{m_{\delta'}}}{I_{Y,2}}\frac{C_{h_\alpha}}{I_{e,1}} \tag{B5}$$

$$E = \left(\frac{C_{m_\alpha}}{I_{Y,1}}\frac{C_{h_\delta}}{I_{e,1}} - \frac{C_{m_\delta}}{I_{Y,1}}\frac{C_{h_\alpha}}{I_{e,1}}\right) + \frac{C_{Z_\alpha}}{m_1}\left[\left(\frac{C_{h_{\theta'}}}{I_{e,2}} + \frac{Vm_e x_e}{I_e}\right)\frac{C_{m_\delta}}{I_{Y,1}} - \frac{C_{m_{\theta'}}}{I_{Y,2}}\frac{C_{h_\delta}}{I_{e,1}}\right] + \frac{C_{Z_\delta}}{m_1}\left[\frac{C_{h_\alpha}}{I_{e,1}}\frac{C_{m_{\theta'}}}{I_{Y,2}} - \left(\frac{C_{h_{\theta'}}}{I_{e,2}} + \frac{Vm_e x_e}{I_e}\right)\frac{C_{m_\alpha}}{I_{Y,1}}\right] \tag{B6}$$

The roots of the characteristic equation are as follows:

For $C_{h_{\delta'}} < \left(C_{h_{\delta'}}\right)_{cr}$,

$$\lambda_{1,2} = a \pm ib$$

which corresponds to the short-period mode of the airframe;

$$\lambda_{3,4} = c \pm id$$

which corresponds to the short-period mode of the elevator; and

$$\lambda_5 = 0$$

which corresponds to indifference of the airframe to pitch attitude.

For $C_{h_{\delta'}} > \left(C_{h_{\delta'}}\right)_{cr}$,

$$\lambda_{1,2} = a \pm ib$$

which corresponds to the short-period mode of the airframe; λ_3 and λ_4 are negative real roots which correspond to the exponential decay of the elevator mode; and

$$\lambda_5 = 0$$

which corresponds to pitch indifference.

APPENDIX C

RESPONSE TO UNIT STEP GUST INPUT

The responses to a unit step gust input are given in terms of the nondimensional penetration distance $s = \frac{Vt}{\bar{c}}$.

For $0 < s < s_p$,

$$a_n(s) = \frac{-C_{Z_{\alpha,WB}}}{m_1} \frac{1}{g} \sin \frac{\pi}{2} \frac{s}{s_p} \tag{C1}$$

$$\theta(s) = 0 \tag{C2}$$

$$\delta(s) = K_2 \left[\frac{-1}{\omega_o K_1} + \left(\frac{1}{\omega_o^2 + K_1^2} \right) \left(\frac{\omega_o}{K_1} e^{\frac{K_1 \bar{c}}{V} s} - \sin \frac{\omega_o \bar{c}}{V} s + \frac{K_1}{\omega_o} \cos \frac{\omega_o \bar{c}}{V} s \right) \right] \tag{C3}$$

For $s_p < s < \infty$ and $C_{h_{\delta'}} < \left(C_{h_\delta}\right)_{cr}$,

$$a_n(s) = \left(\frac{-C_{Z_\alpha}}{m_1} \frac{V}{g} \right) \left\{ e^{\alpha_1 (s - s_p)} \left[A_1 \cos \beta (s - s_p) + B_1 \sin \beta (s - s_p) \right] + e^{\alpha_2 (s - s_p)} \left[C_1 \cos \Delta (s - s_p) + D_1 \sin \Delta (s - s_p) \right] \right\} \tag{C4}$$

$$\theta(s) = \left\{ e^{\alpha_1 (s - s_p)} \left[A_2 \cos \beta (s - s_p) + B_2 \sin \beta (s - s_p) \right] + e^{\alpha_2 (s - s_p)} \left[C_2 \cos \Delta (s - s_p) + D_2 \sin \Delta (s - s_p) \right] \right\} + E_2 \tag{C5}$$

$$\delta(s) = e^{\alpha_1(s-s_p)}\left[A_3 \cos \beta(s - s_p) + B_3 \sin \beta(s - s_p)\right] + e^{\alpha_2(s-s_p)}\left[C_3 \cos \Delta(s - s_p) + D_3 \sin \Delta(s - s_p)\right] \quad (C6)$$

For $s_p < s < \infty$ and $C_{h_{\delta'}} > \left(C_{h_{\delta'}}\right)_{cr}$,

$$a_n(s) = \left(\frac{-C_{Z_\alpha}}{m_1}\frac{V}{g}\right)\left\{e^{\alpha_1(s-s_p)}\left[A_1 \cos \beta(s - s_p) + B_1 \sin \beta(s - s_p)\right] + C_1 e^{\alpha_3(s-s_p)} + D_1 e^{\alpha_4(s-s_p)}\right\} \quad (C7)$$

$$\theta(s) = e^{\alpha_1(s-s_p)}\left[A_2 \cos \beta(s - s_p) + B_2 \sin \beta(s - s_p)\right] + C_2 e^{\alpha_3(s-s_p)} + D_2 e^{\alpha_4(s-s_p)} + E_2 \quad (C8)$$

$$\delta(s) = e^{\alpha_1(s-s_p)}\left[A_3 \cos \beta(s - s_p) + B_3 \sin \beta(s - s_p)\right] + C_3 e^{\alpha_3(s-s_p)} + D_3 e^{\alpha_4(s-s_p)} \quad (C9)$$

It should be pointed out that the arbitrary constants are A_1, B_1, C_1, D_1, and E_2. The remaining constants, A_2, A_3, B_2, B_3, C_2, C_3, D_2, and D_3 are the modal constants and are linear functions of the arbitrary constants and the stability derivatives, mass parameters, and flight conditions. These constants were determined by standard mathematical techniques.

APPENDIX D

RESPONSE TO CONTINUOUS GUSTS

The normal-acceleration response of the airplane to an infinitely long succession of gusts of the form

$$\alpha_g = \frac{1}{V} \sin \omega_g t = \frac{1}{V} \sin\left(\frac{\nu V}{\frac{b}{c}}\right)t \tag{D1}$$

is given by the following equation for $C_{h_{\delta'}} < (C_{h_{\delta'}})_{cr}$:

$$\frac{\frac{F_n(i\nu)}{-C_{Z_\alpha} V}}{\frac{m_1}{\rho}} = \frac{C_{Z_{\alpha,WB}}}{C_{Z_\alpha}} \frac{1}{V} \left\{ \frac{\nu}{\omega_s^2 - \nu^2} \left[\nu \cos \nu s_p + i(\omega_s - \nu \sin \nu s_p) \right] \right\} +$$

$$A_1 \left(\frac{\nu}{\nu^4 + 2(\alpha_1^2 - \beta^2)\nu^2 + (\alpha_1^2 + \beta^2)^2} \left\{ \left[\nu(\alpha_1^2 - \beta^2 + \nu^2) \cos \nu s_p + (-\alpha_1)(\alpha_1^2 + \beta^2 + \nu^2) \sin \nu s_p \right] + \right. \right.$$

$$\left. \left. i\left[-\nu(\alpha_1^2 - \beta^2 + \nu^2) \sin \nu s_p + (-\alpha_1)(\alpha_1^2 + \beta^2 + \nu^2) \cos \nu s_p \right] \right\} \right) +$$

$$B_1 \left(\frac{\nu\beta}{\nu^4 + 2(\alpha_1^2 - \beta^2)\nu^2 + (\alpha_1^2 + \beta^2)^2} \left\{ \left[\nu(-2\alpha_1) \cos \nu s_p + (\alpha_1^2 + \beta^2 - \nu^2) \sin \nu s_p \right] + \right. \right.$$

$$\left. \left. i\left[-\nu(-2\alpha_1) \sin \nu s_p + (\alpha_1^2 + \beta^2 - \nu^2) \cos \nu s_p \right] \right\} \right) +$$

$$C_1 \left(\frac{\nu}{\nu^4 + 2(\alpha_2^2 - \Delta^2)\nu^2 + (\alpha_2^2 + \Delta^2)^2} \left\{ \left[\nu(\alpha_2^2 - \Delta^2 + \nu^2) \cos \nu s_p + (-\alpha_2)(\alpha_2^2 + \Delta^2 + \nu^2) \sin \nu s_p \right] + \right. \right.$$

$$\left. \left. i\left[-\nu(\alpha_2^2 - \Delta^2 + \nu^2) \sin \nu s_p + (-\alpha_2)(\alpha_2^2 + \Delta^2 + \nu^2) \cos \nu s_p \right] \right\} \right) +$$

$$D_1 \left(\frac{\nu\Delta}{\nu^4 + 2(\alpha_2^2 - \Delta^2)\nu^2 + (\alpha_2^2 + \Delta^2)^2} \left\{ \left[\nu(-2\alpha_2) \cos \nu s_p + (\alpha_2^2 + \Delta^2 - \nu^2) \sin \nu s_p \right] + \right. \right.$$

$$\left. \left. i\left[-\nu(-2\alpha_2) \sin \nu s_p + (\alpha_2^2 + \Delta^2 - \nu^2) \cos \nu s_p \right] \right\} \right) \tag{D2}$$

For $C_{h_{\delta'}} > \left(C_{h_{\delta'}}\right)_{cr}$, the expression for $F_n(i\nu)$ is modified only in the C_1 and D_1 terms. These terms now become

$$C_1\left(\frac{\nu}{\nu^2 + \alpha_3{}^2}\left\{\left[\nu \cos \nu s_p + \left(-\alpha_3\right)\sin \nu s_p\right] + i\left[-\nu \sin \nu s_p + \left(-\alpha_3\right)\cos \nu s_p\right]\right\}\right) \tag{D3}$$

and

$$D_1\left(\frac{\nu}{\nu^2 + \alpha_4{}^2}\left\{\left[\nu \cos \nu s_p + \left(-\alpha_4\right)\sin \nu s_p\right] + i\left[-\nu \sin \nu s_p + \left(-\alpha_4\right)\cos \nu s_p\right]\right\}\right) \tag{D4}$$

In either case, the initial term

$$\frac{\nu}{\omega_s{}^2 - \nu^2}\left[\nu \cos \nu s_p + i\left(\omega_s - \nu \sin \nu s_p\right)\right] = \frac{\pi}{4} + \frac{i}{2}$$

when $\omega_s = \nu$.

REFERENCES

1. Donely, Philip: Summary of Information Relating to Gust Loads on Airplanes. NACA Rep. 997, 1950. (Supersedes NACA TN 1976.)

2. Press, Harry, and Mazelsky, Bernard: A Study of the Application of Power-Spectral Methods of Generalized Harmonic Analysis to Gust Loads on Airplanes. NACA Rep. 1172, 1954. (Supersedes NACA TN 2853.)

3. Croom, Delwin R., Shufflebarger, C. C., and Huffman, Jarrett K.: An Investigation of Forward-Located Fixed Spoilers and Deflectors as Gust Alleviators on an Unswept-Wing Model. NACA TN 3705, 1956.

4. Rea, James B.: Dynamic Analysis of Aeroelastic Aircraft by the Transfer Function-Fourier Method. Rep. SM-13868, Douglas Aircraft Co., Inc., July 13, 1950.

5. Brooks, Billy S., and Miller, Glenn C.: An Analysis of the Effectiveness of a Gust Alleviating Device. Tech. Note WCLS 53-52, Wright Air Dev. Center, U. S. Air Force, July 1, 1953.

6. Ludwig, L. G.: Final Internal Research Report - A Proposed Gust Alleviation System for Aircraft. Rep. No. SB-653-S-2, Cornell Aero. Lab., Inc., Feb. 1950.

7. Phillips, William H., and Kraft, Christopher C., Jr.: Theoretical Study of Some Methods for Increasing the Smoothness of Flight Through Rough Air. NACA TN 2416, 1951.

8. Boucher, Robert W., and Kraft, Christopher C., Jr.: Analysis of a Vane-Controlled Gust-Alleviation System. NACA TN 3597, 1956.

9. Kraft, Christopher C., Jr.: Initial Results of a Flight Investigation of a Gust-Alleviation System. NACA TN 3612, 1956.

10. Schindler, Martin H.: An Analytical Study of the Gust-Load Alleviation Obtained by Means of a Normal-Acceleration-Controlled Flap. M. S. of A. E. Thesis, Univ. of Virginia, 1952.

11. Payne, Chester B.: A Flight Investigation of Some Effects of Automatic Control on Gust Loads. NACA RM L53E14a, 1953.

12. Crane, Harold L., Hurt, George J., Jr., and Elliott, John M.: Subsonic Flight Investigation of Methods To Improve the Damping of Lateral Oscillations by Means of a Viscous Damper in the Rudder System in Conjunction With Adjusted Hinge-Moment Parameters. NACA RM L54D09, 1954.

13. Mazelsky, Bernard, and Diederich, Franklin W.: A Method of Determining the Effect of Airplane Stability on the Gust Load Factor. NACA TN 2035, 1950.

14. Brenner, Claude W., and Isakson, Gabriel: A Parametric Investigation of Gust Loads on Rigid Airplanes in Two Degrees of Freedom. Bur. Aero. Contract No. NOa(s)51-183-C, M.I.T. Aeroelastics and Structures Res. Lab., Oct. 6, 1952.

15. Vitale, A. James, Press, H., and Shufflebarger, C. C.: An Investigation of the Use of Rocket-Powered Models for Gust-Load Studies With an Application to a Tailless Swept-Wing Model at Transonic Speeds. NACA TN 3161, 1954.

16. Spreemann, Kenneth P., and Alford, William J., Jr.: Investigation of the Effects of Leading-Edge Flaps on the Aerodynamic Characteristics in Pitch at Mach Numbers From 0.40 to 0.93 of a Wing-Fuselage Configuration With a 45° Sweptback Wing of Aspect Ratio 4. NACA RM L53G13, 1953.

17. Turner, Thomas R.: Effects of Rate of Flap Deflection on Flap Hinge Moment and Wing Lift Through the Mach Number Range From 0.32 to 0.87. NACA RM L53E11, 1953.

TABLE I.- PERTINENT AIRPLANE CHARACTERISTICS

Geometric characteristics:

	Wing	Stabilizer	Elevator[a]
S, sq ft	3.77	0.565	0.10
$\bar{c}$, ft	1.068	0.384	0.0895
Aspect ratio	4.0	4.0	------
Sweepback, deg	[b]45.0	[b]7.13	[c]0
Taper ratio, deg	0.300	0.600	0.665
Distance from center of gravity to 0.25 mean aerodynamic chord, ft	0	2.31	[d]2.50

Mass characteristics:

m, slugs	3.00
m_e, slugs	0.0264
I_Y, slug-ft^2	6.60
$I_{Y,e}$, slug-ft^2	0.000293
x_e/c_e	-0.3366

Flight conditions:

Altitude, ft	0
Static pressure, lb/sq ft	2,116
Velocity of sound, ft/sec	1,116
M_∞	0.7
q_∞, lb/sq ft	725
V, ft/sec	780

Aerodynamic characteristics:

C_{Z_α}	-4.25	C_{m_θ}	-4.15
C_{Z_δ}	0	$C_{m_{\dot{\delta}}}$	0
$C_{Z_{\alpha,WB}}$	-3.87	C_{h_α}	-0.100
s_p, wing chords	4	C_{h_δ}	-0.484
C_{m_α}	-1.162	$C_{h_{\dot{\alpha}}}$	-1.95
C_{m_δ}	-0.556	C_{h_θ}	-5.28
$C_{m_{\dot{\alpha}}}$	-0.87	$C_{h_{\dot{\delta}}}$	0 to $-\infty$

[a]All calculations based on exposed elevator area.

[b]At quarter-chord line.

[c]At hinge line.

[d]Distance from center of gravity to elevator hinge axis.

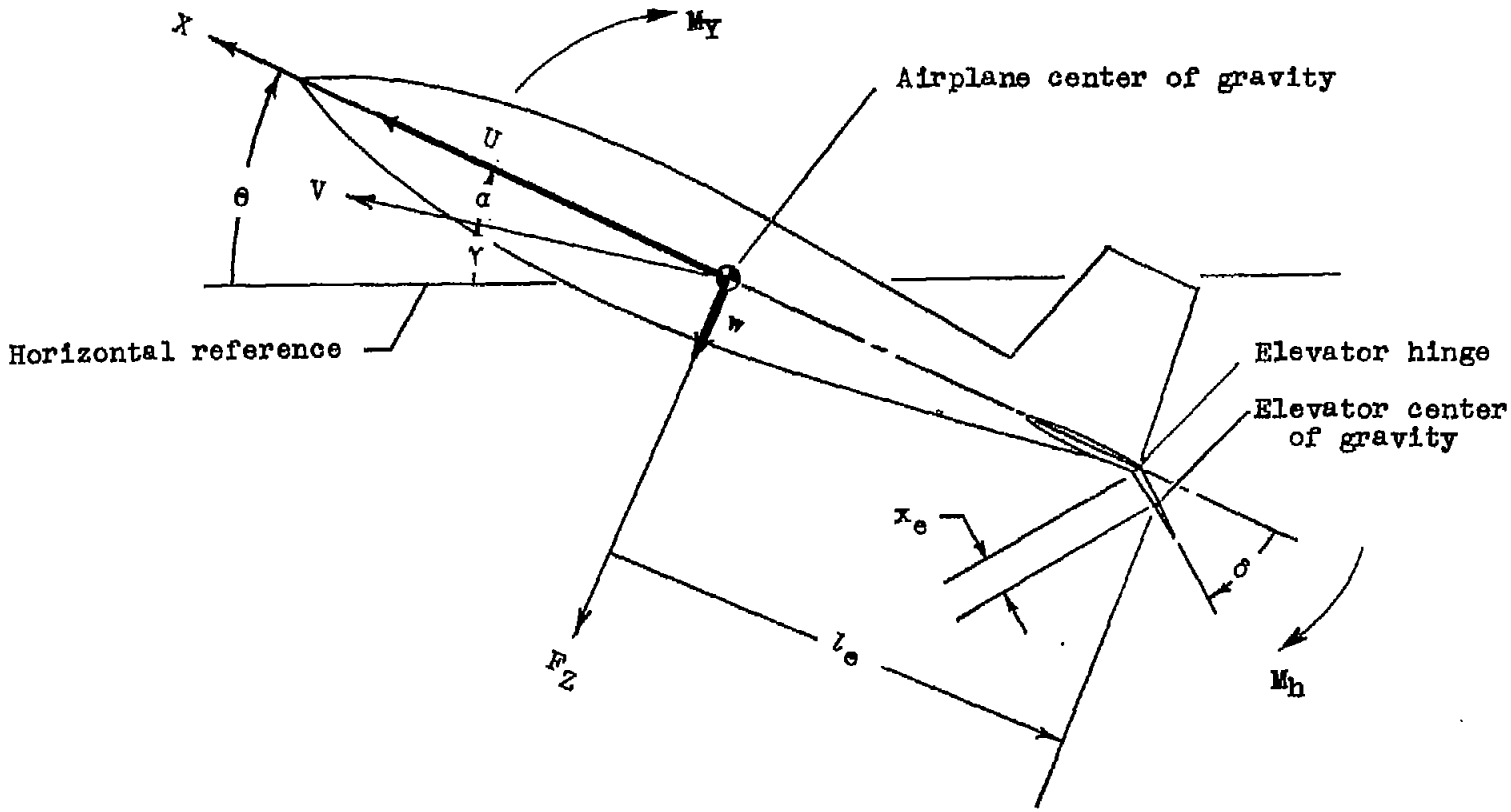

Figure 1.- Body-axis system used in analysis. Axes remain fixed relative to airplane.

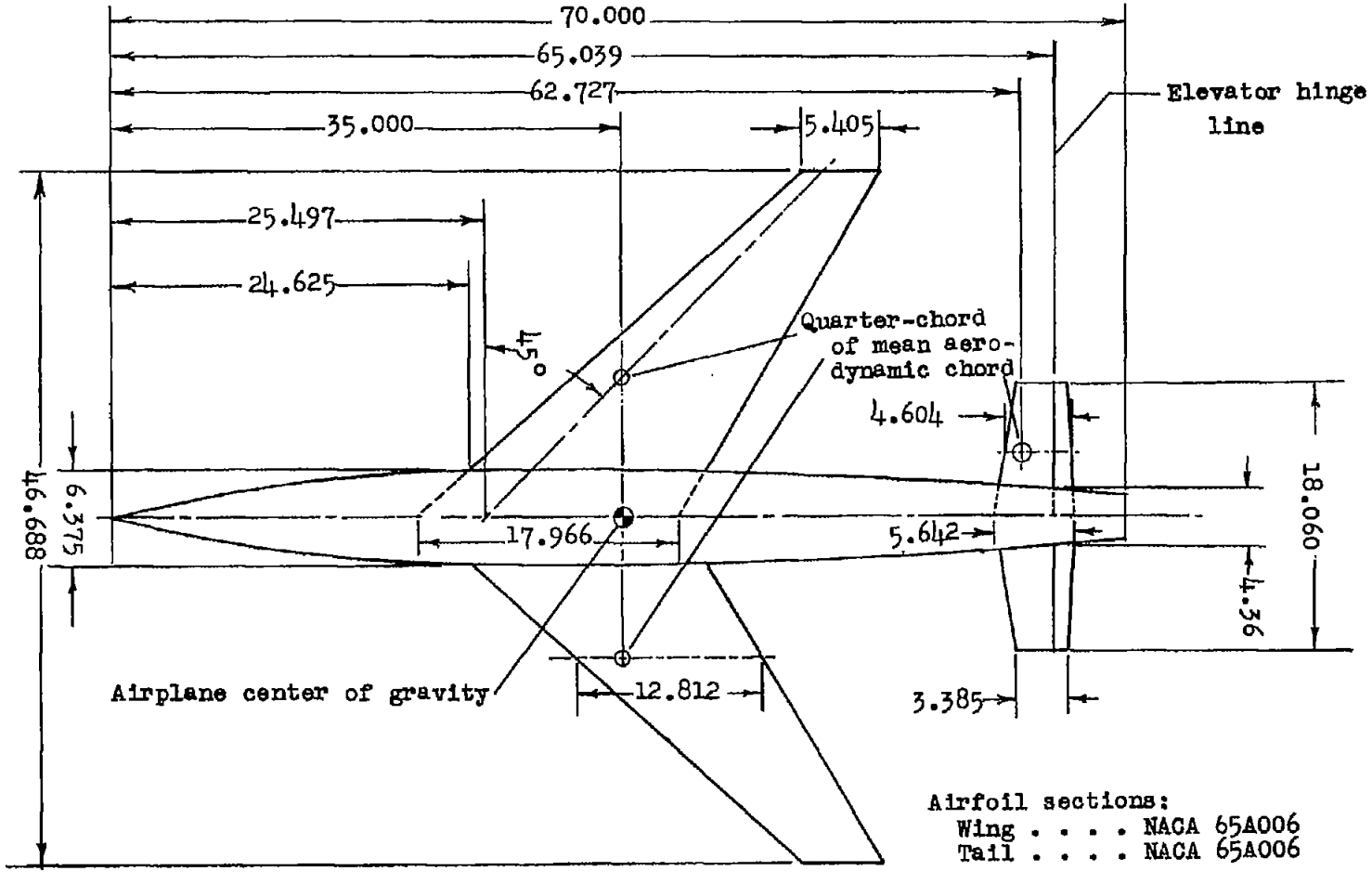

Figure 2.- Outline sketch of airplane. All dimensions are in inches.

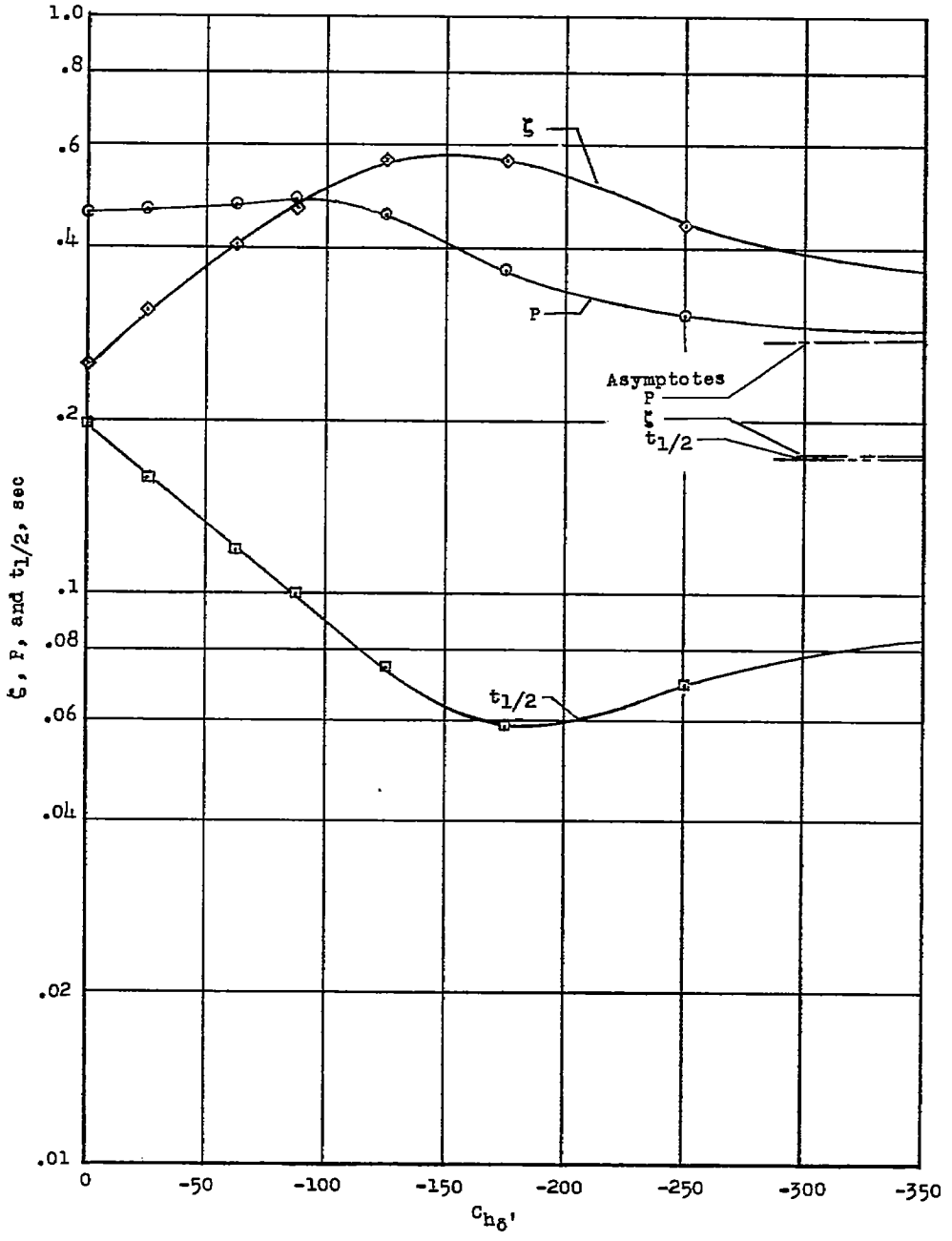

(a) Airframe mode.

Figure 3.- Effect of $C_{h'_\delta}$ on dynamic stability of classical free oscillation.

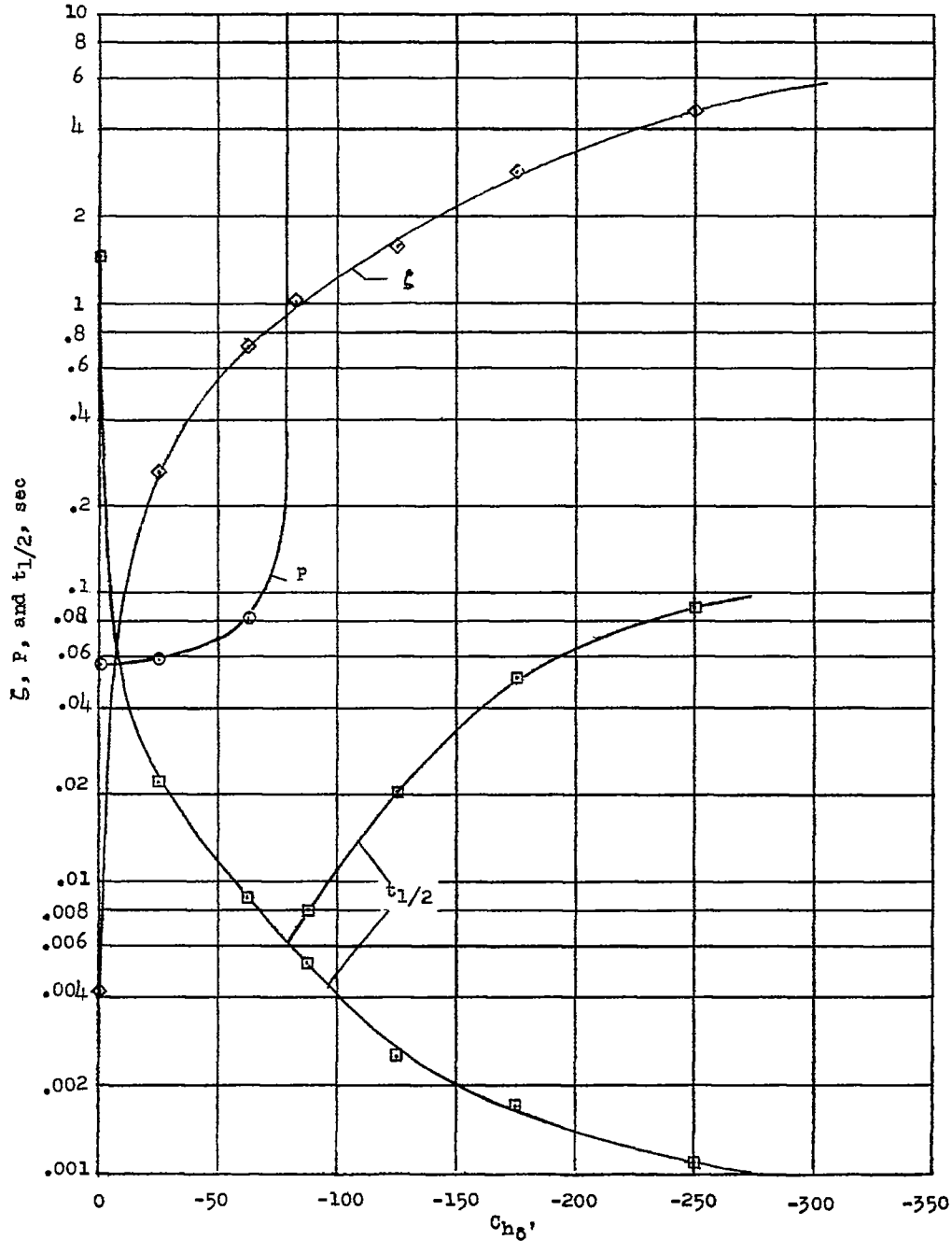

(b) Elevator mode.

Figure 3.- Concluded.

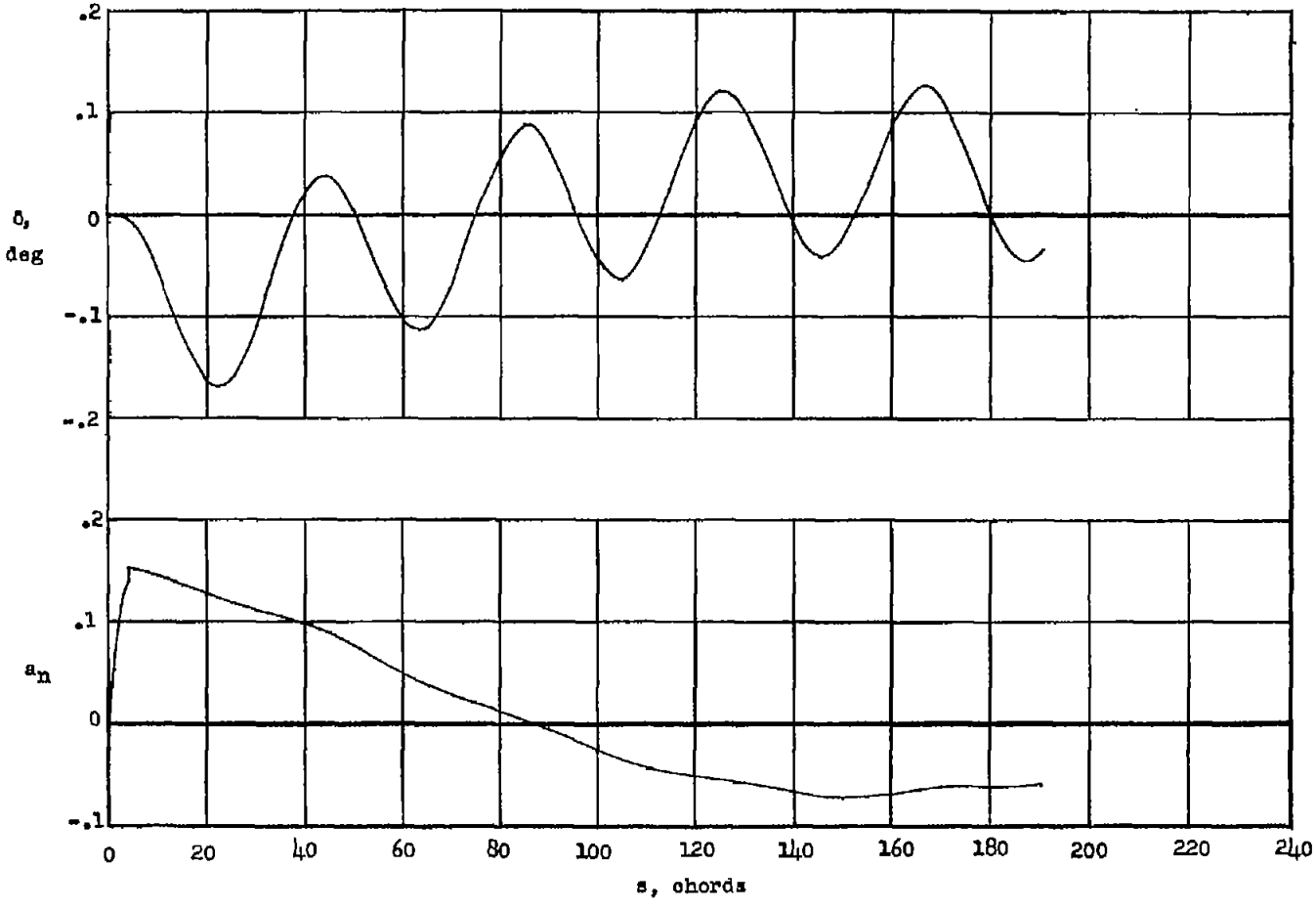

(a) $C_{h_{\delta'}} = 0.$

Figure 4.- Gust indicial responses.

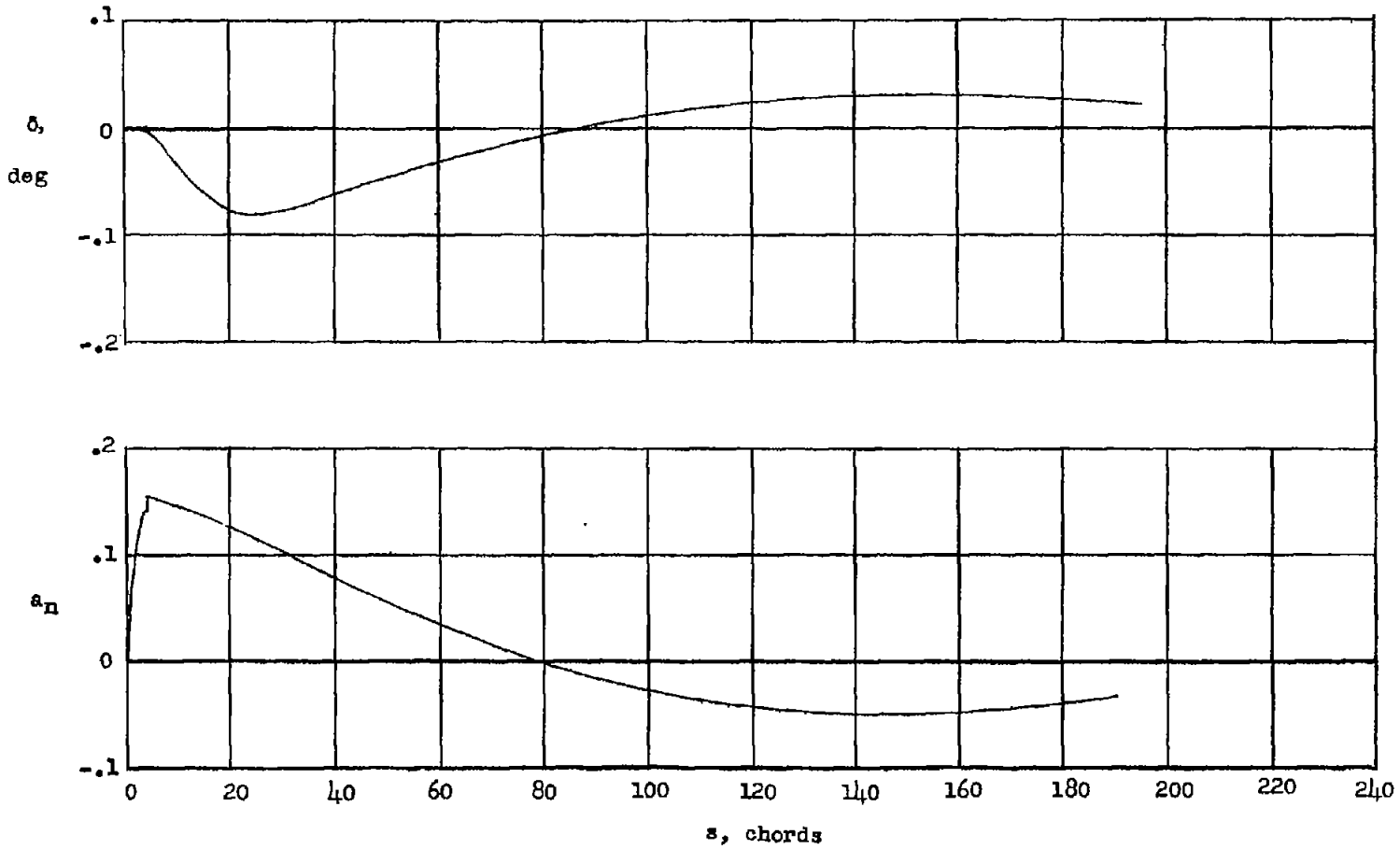

(b) $C_{h_{\delta'}} = -62.5$.

Figure 4.- Continued.

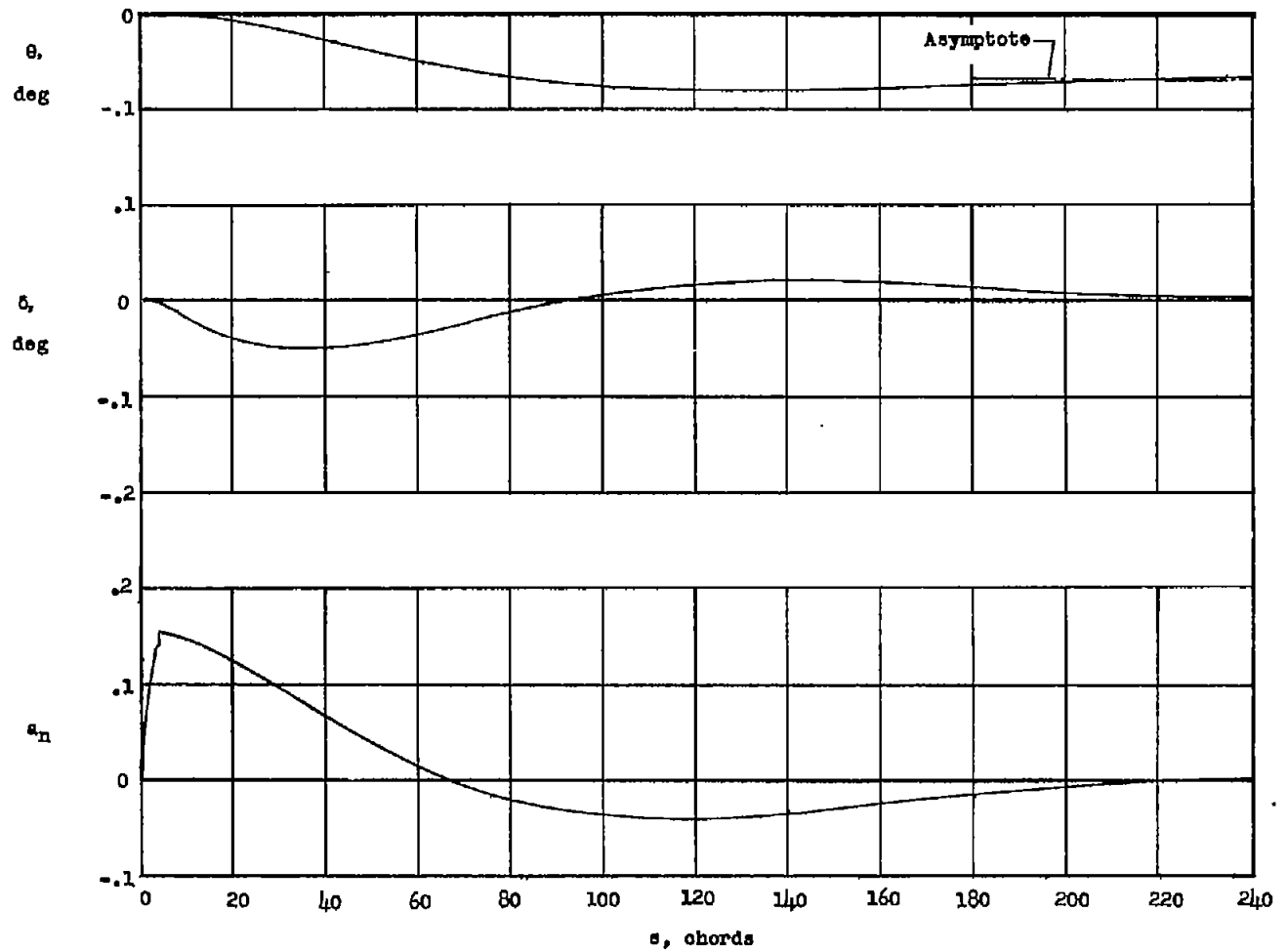

(c) C_{h_δ}, = -175.

Figure 4.- Continued.

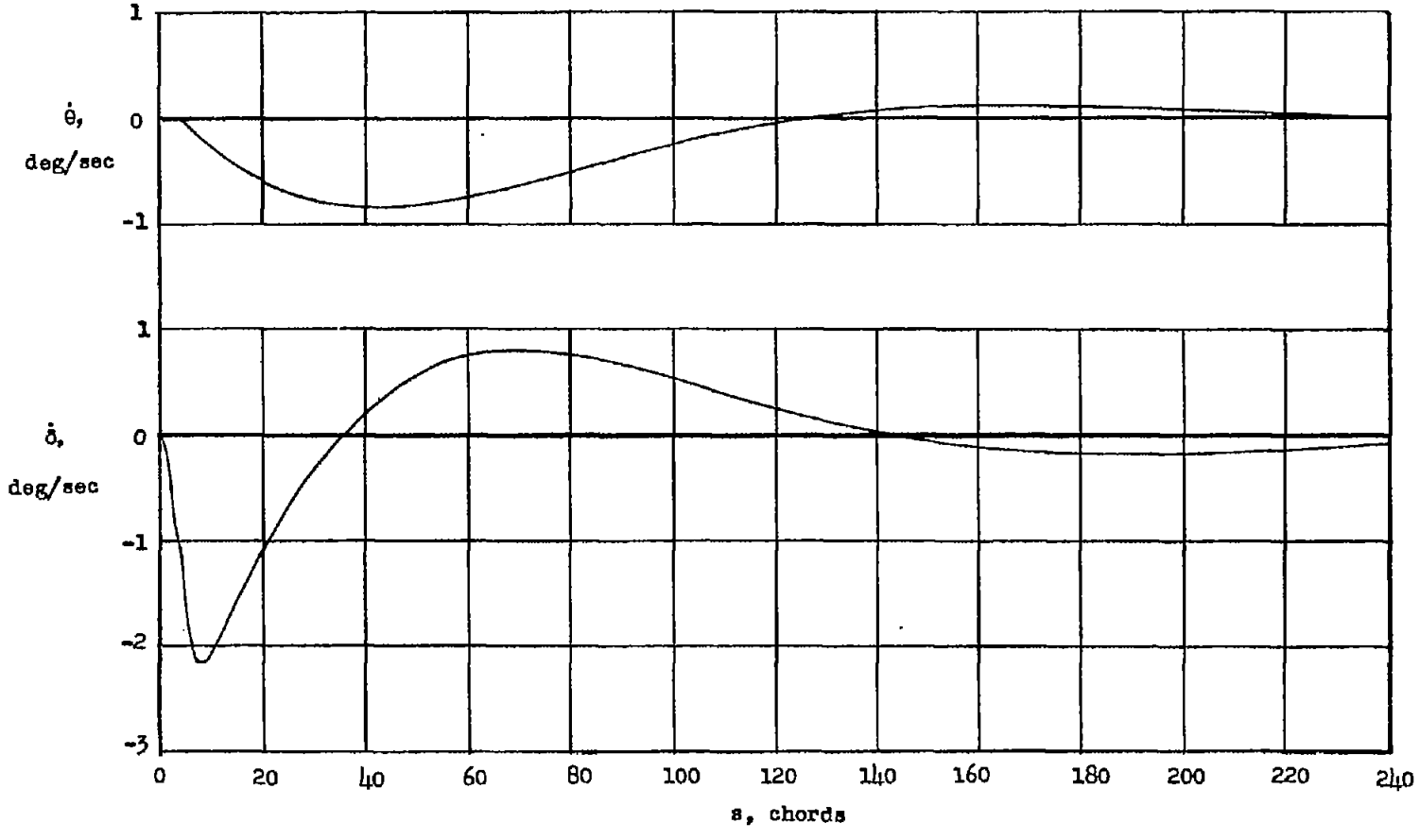

(d) $C_{h_{\dot{\delta}}} = -175.$

Figure 4.- Continued.

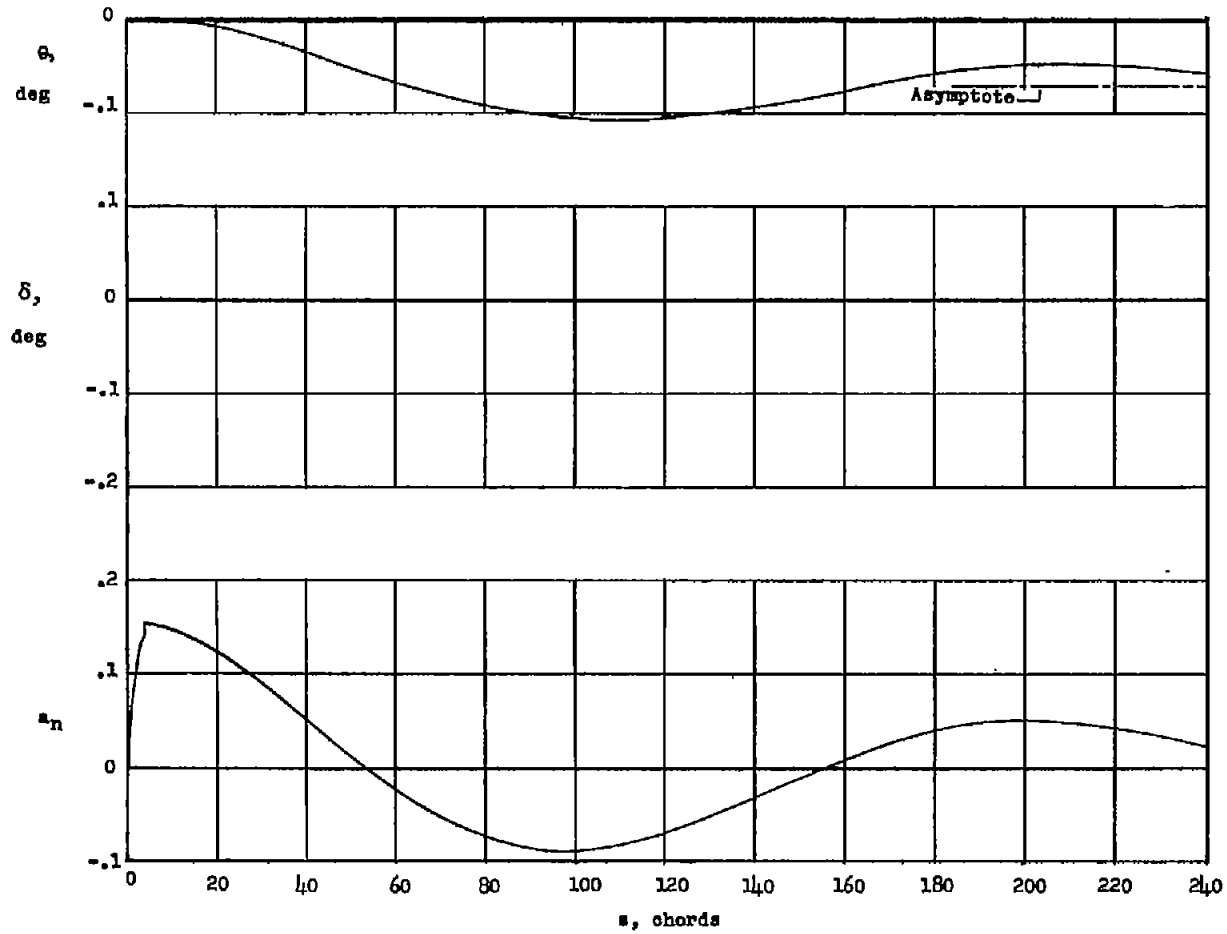

(e) C_{h_δ}, = $-\infty$.

Figure 4.- Continued.

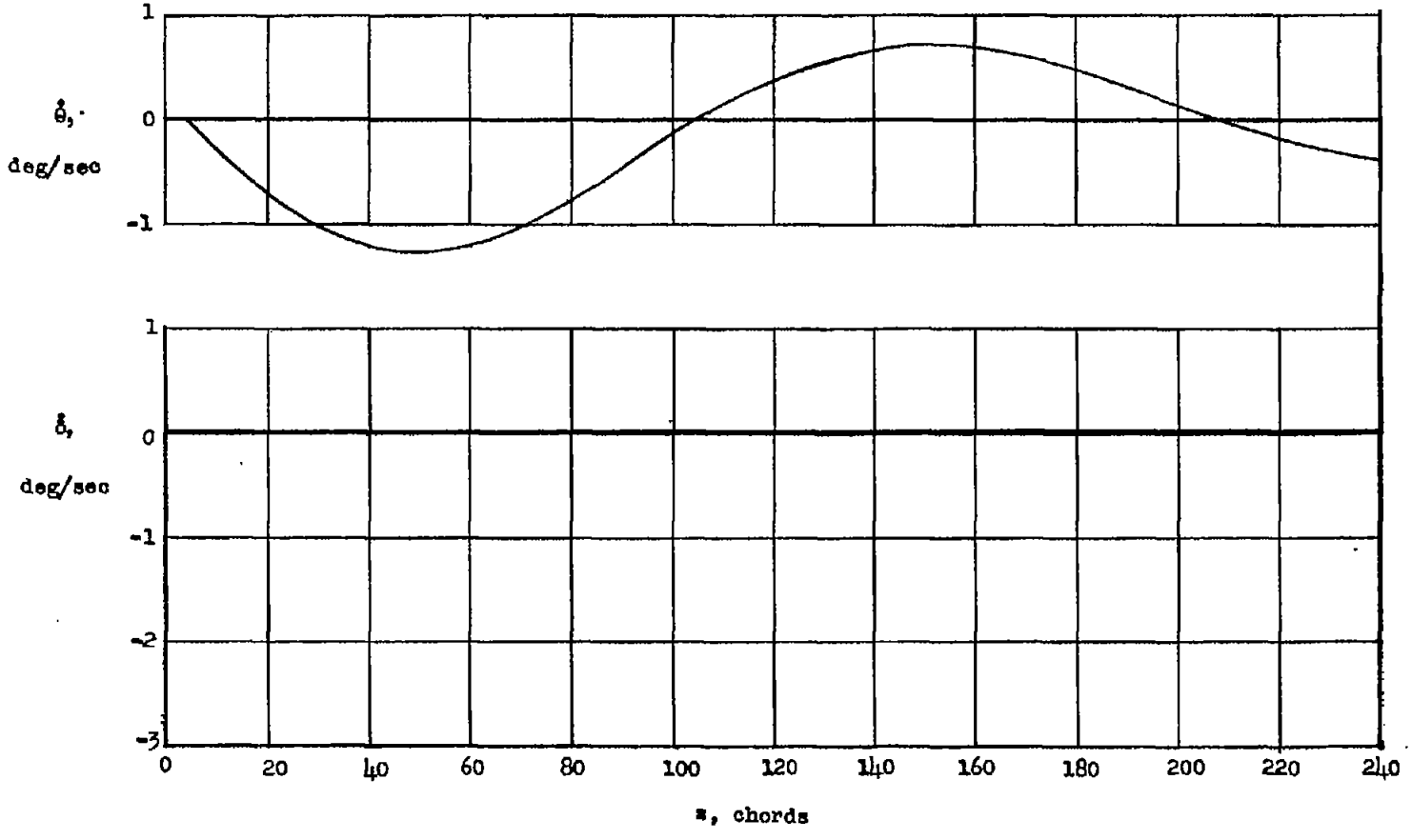

(f) $C_{h_{\dot{\delta}}} = -\infty$.

Figure 4.- Concluded.

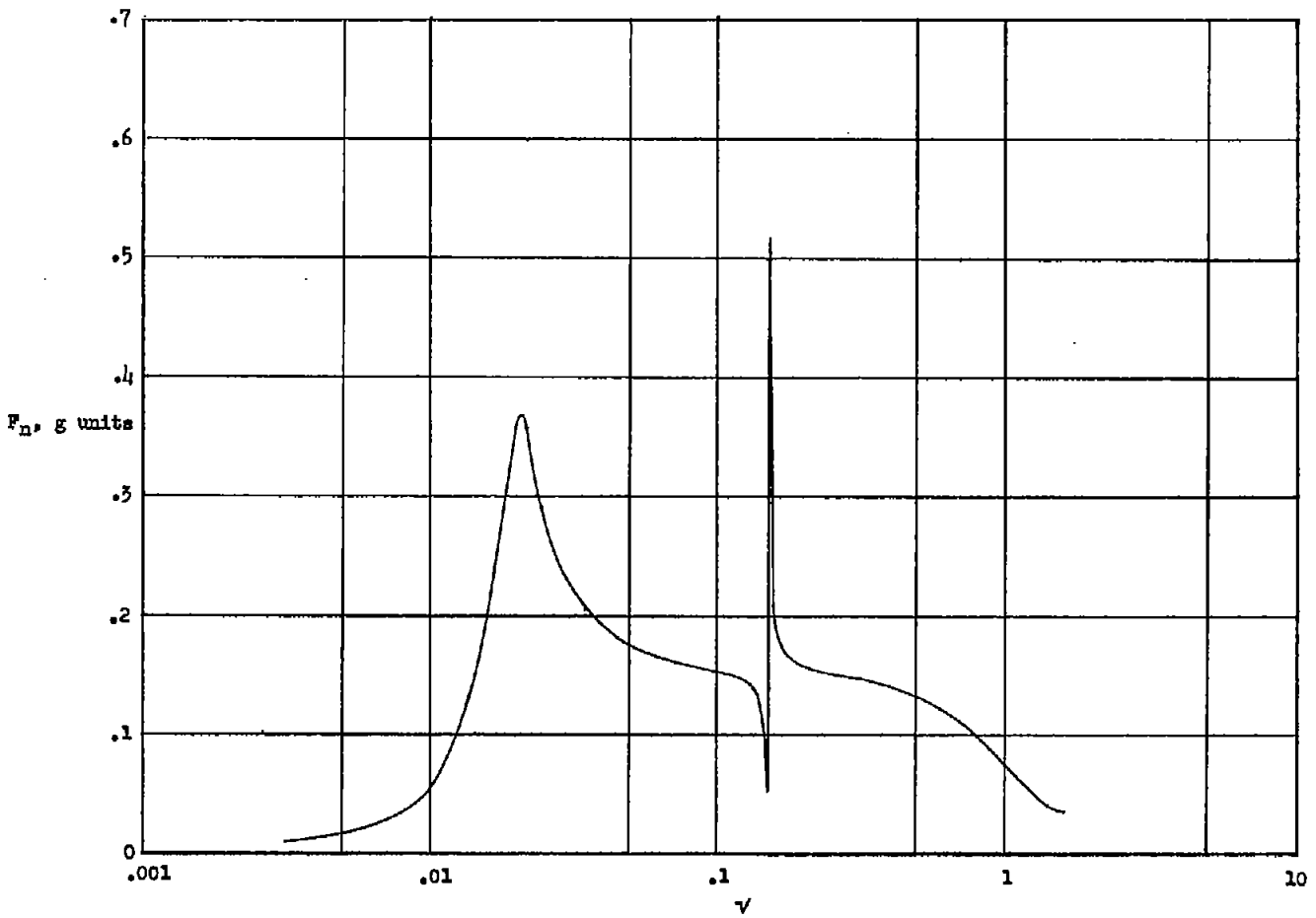

(a) C_{h_δ}, = 0.

Figure 5.- Normal-acceleration gust-frequency-response functions.

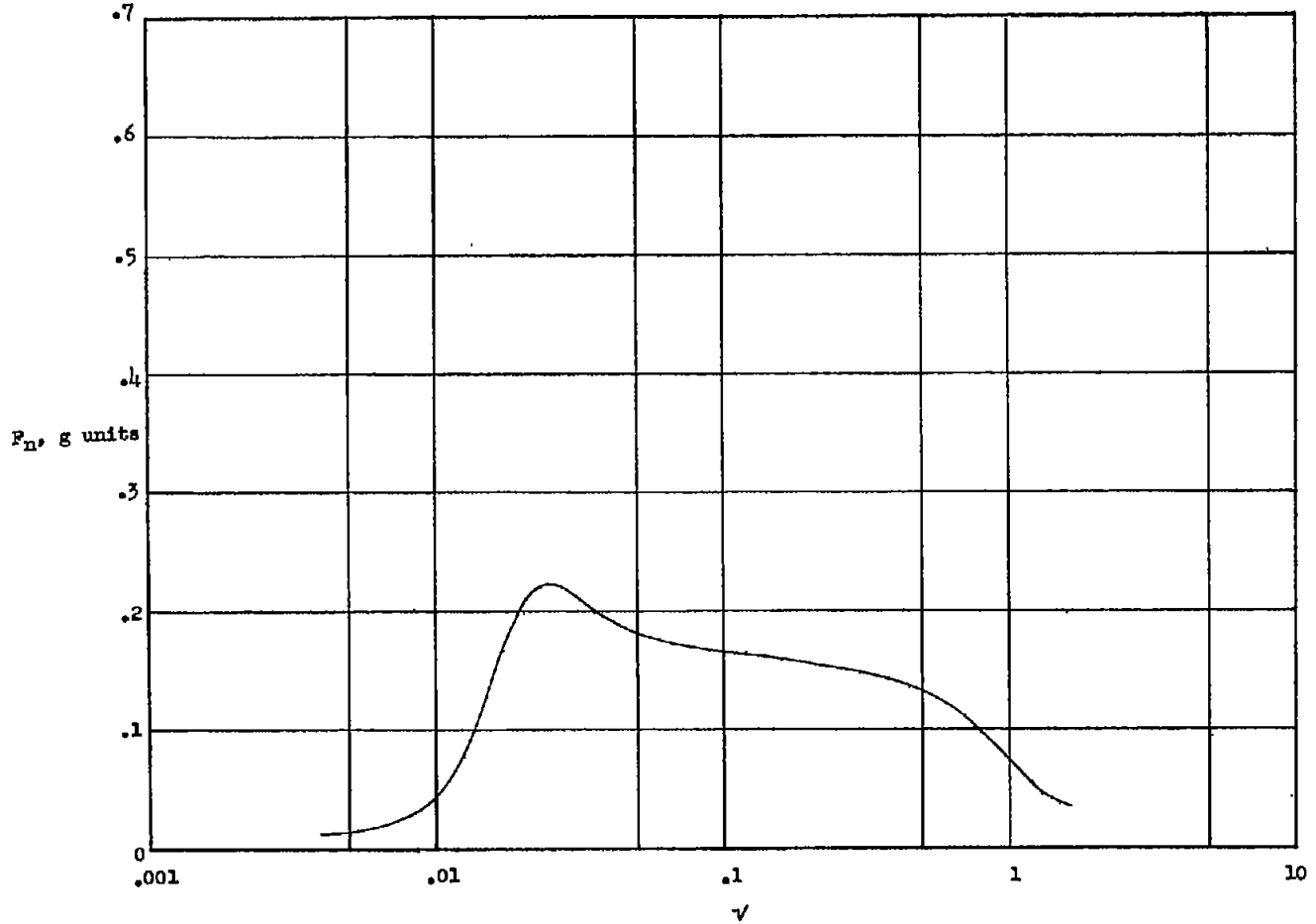

(b) $C_{h_\delta} = -62.5$.

Figure 5.- Continued.

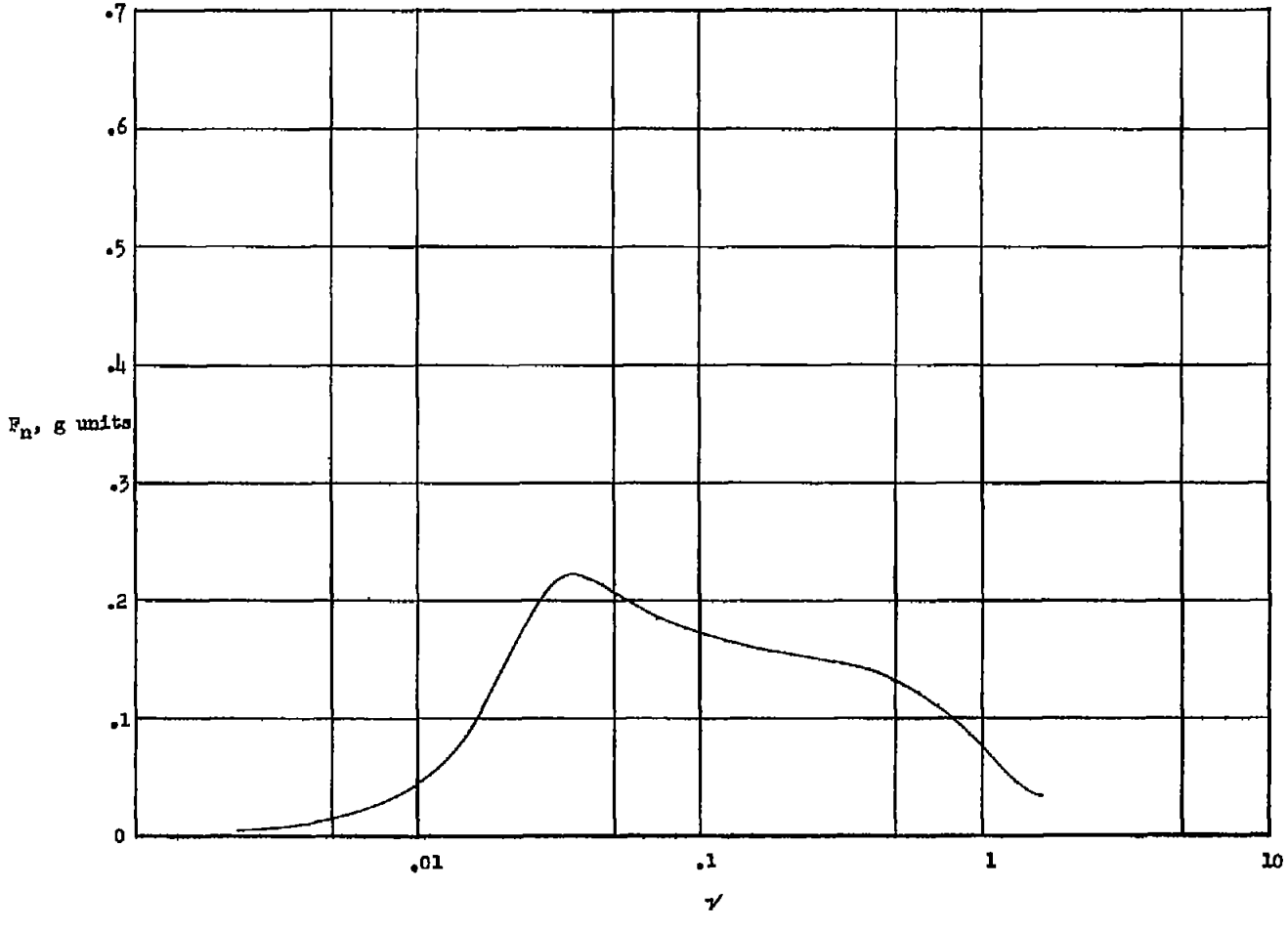

(c) C_{h_δ}, = -175.

Figure 5.- Continued.

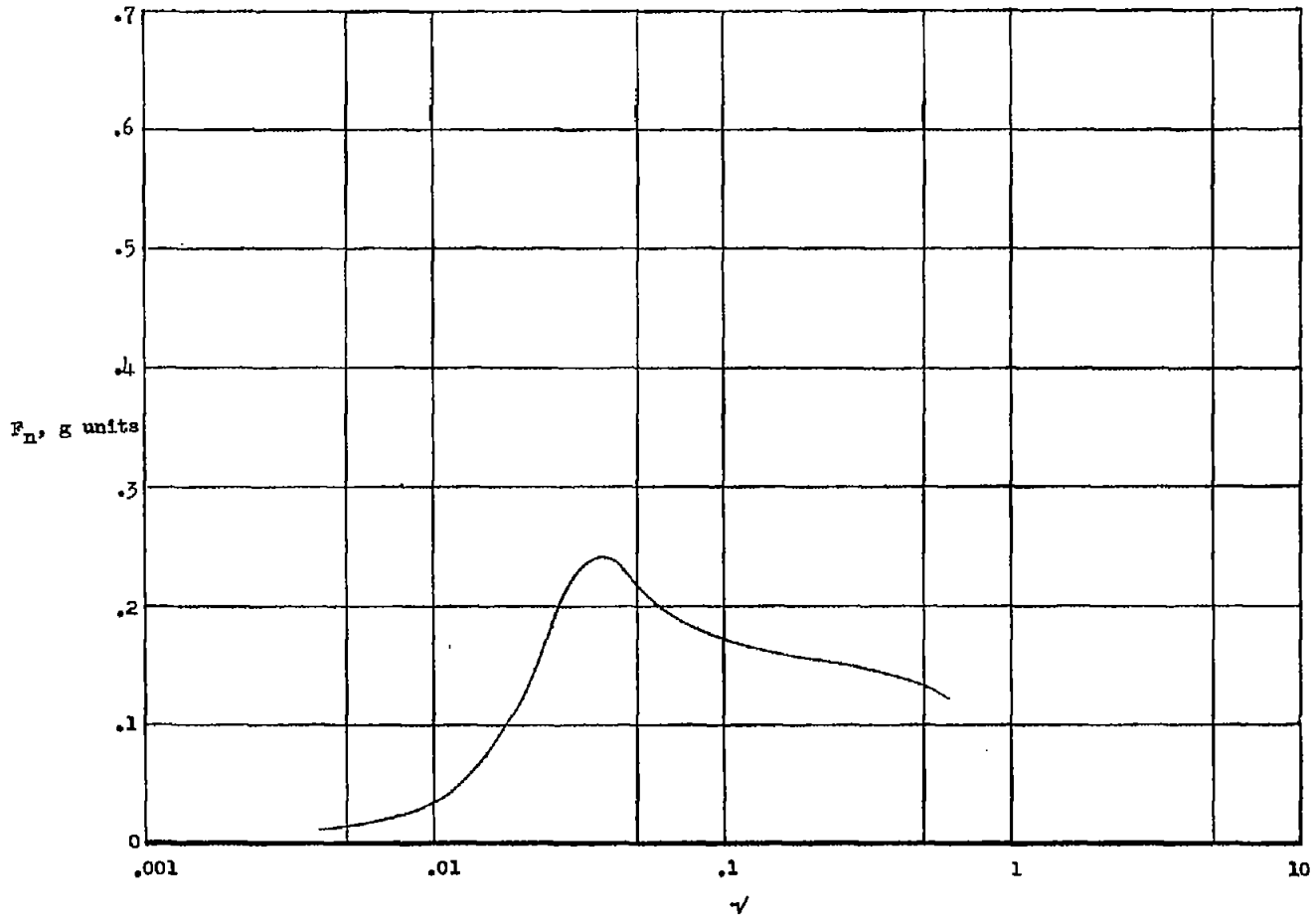

(d) $C_{h_{\delta'}} = -250.$

Figure 5.- Continued.

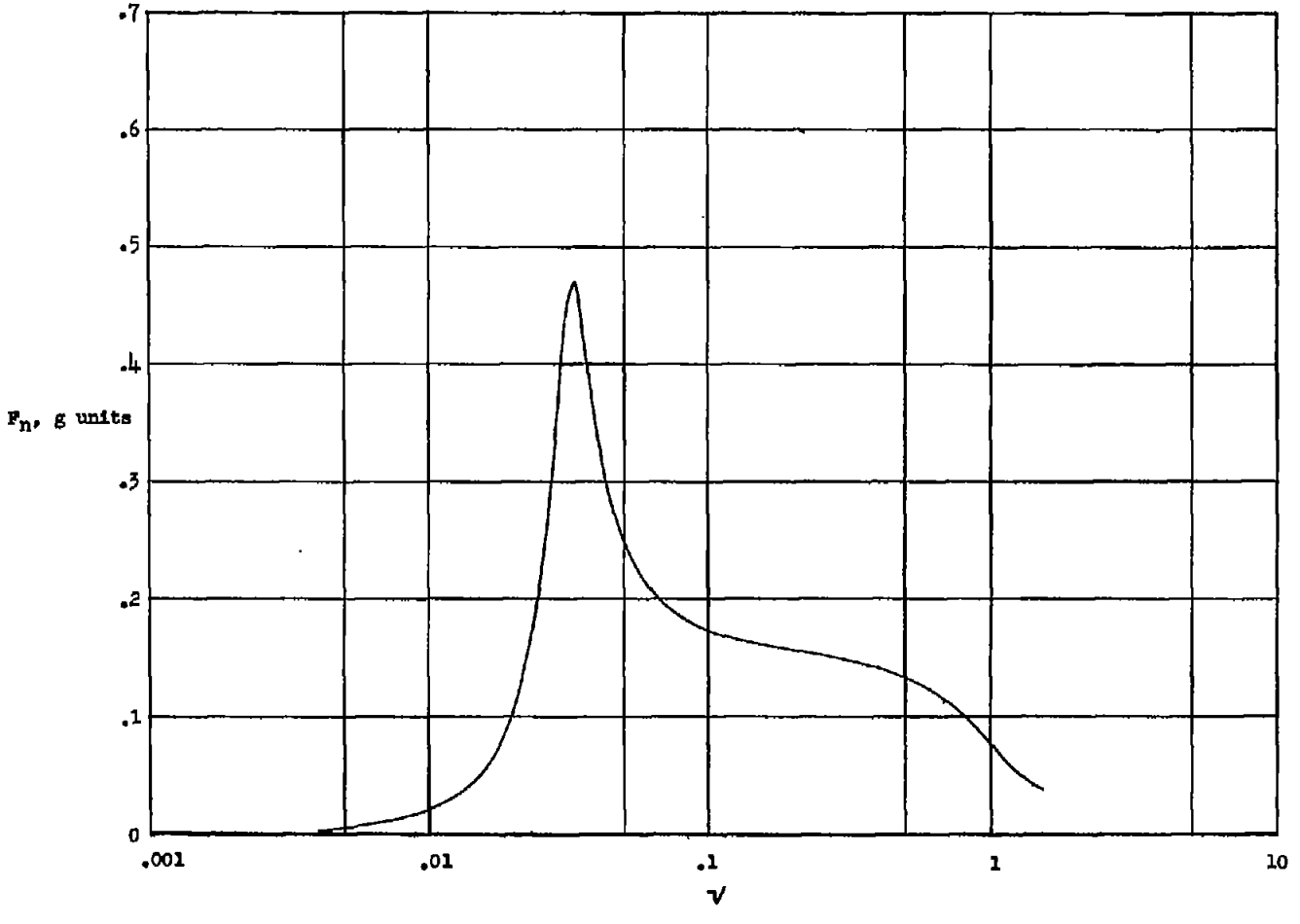

(e) $C_{h_{\delta'}} = -\infty$.

Figure 5.- Concluded.

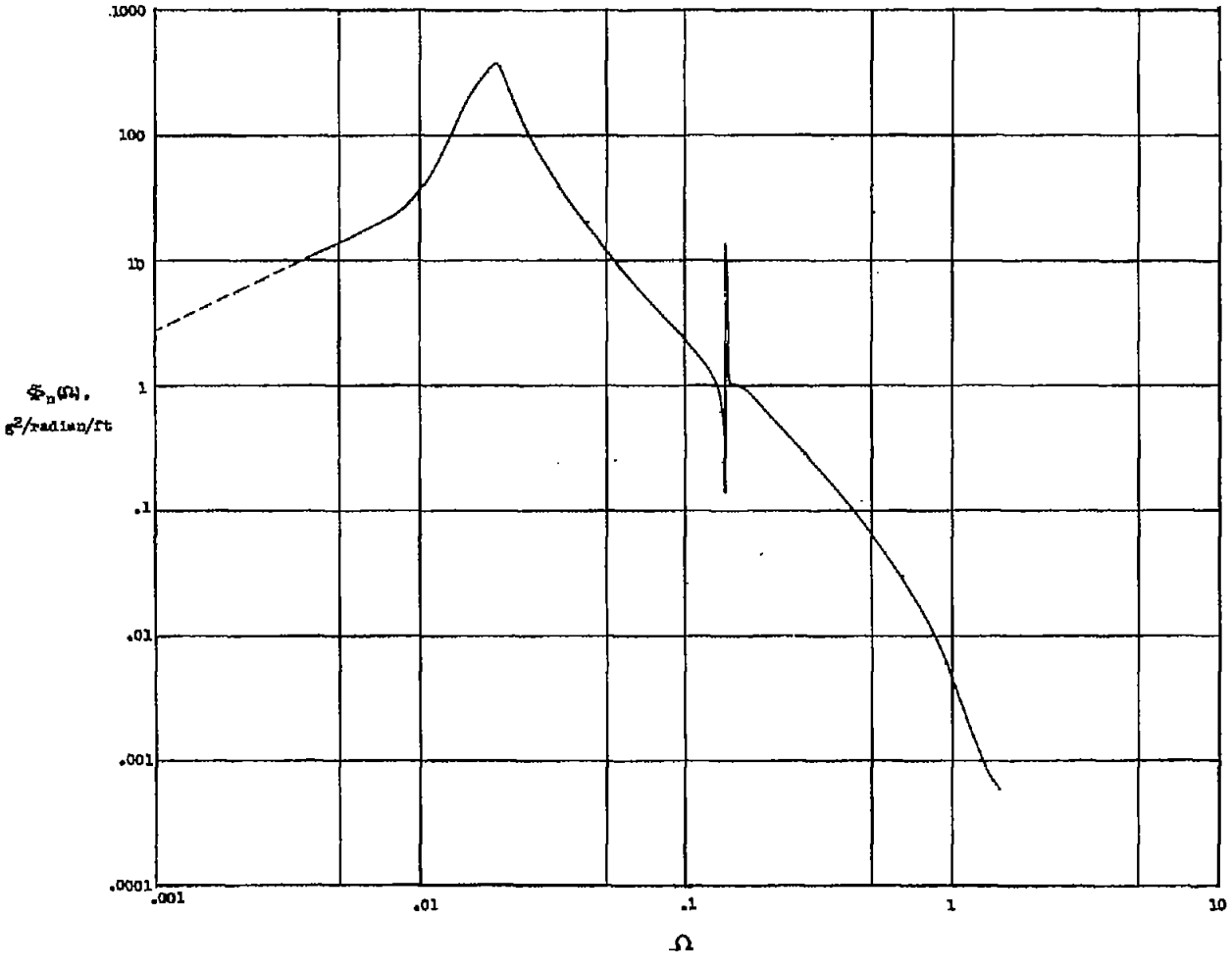

(a) $C_{h_{\delta'}} = 0.$

Figure 6.- Power-spectral-density function of normal-acceleration response.

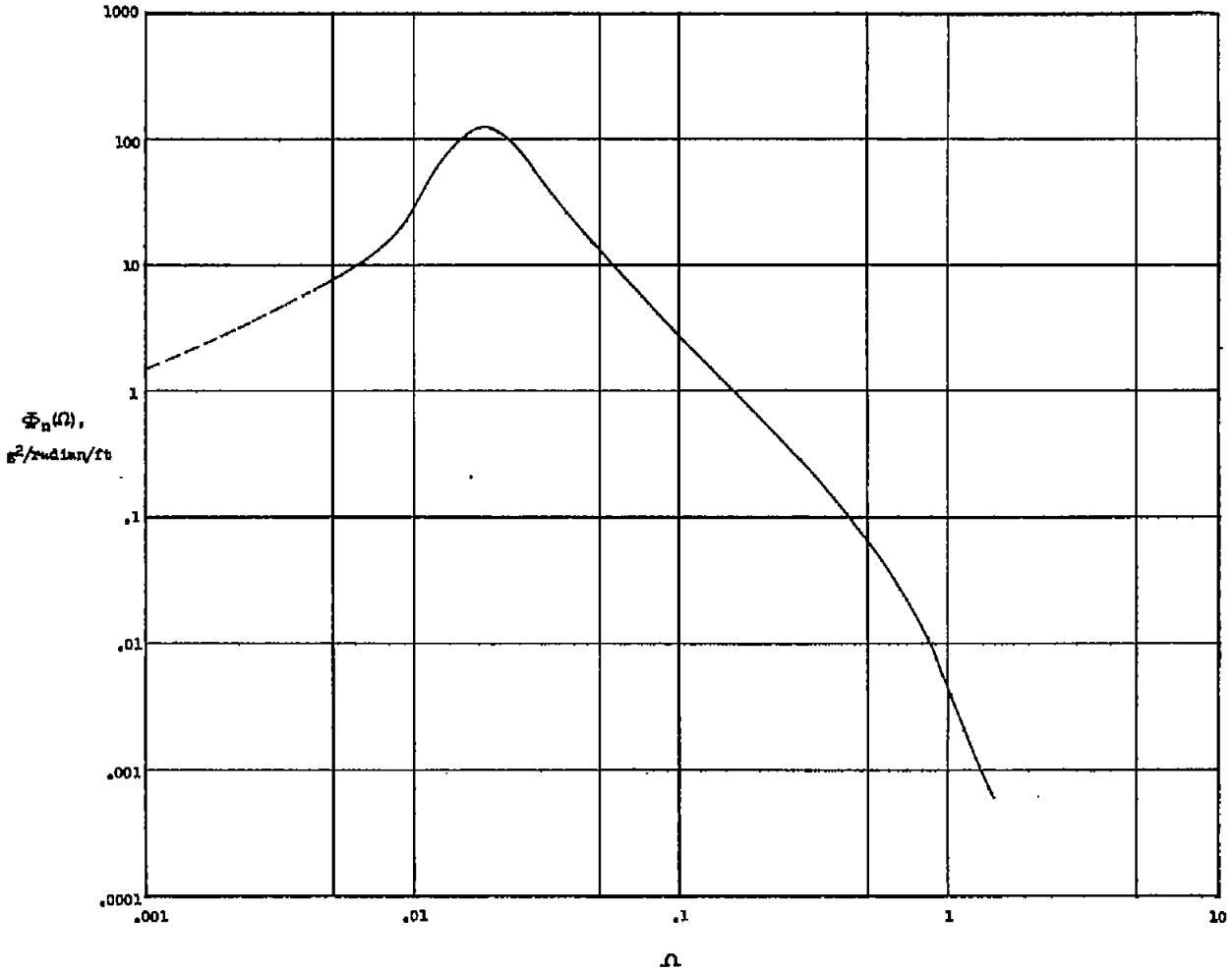

(b) C_{h_δ}, = -62.5.

Figure 6.- Continued.

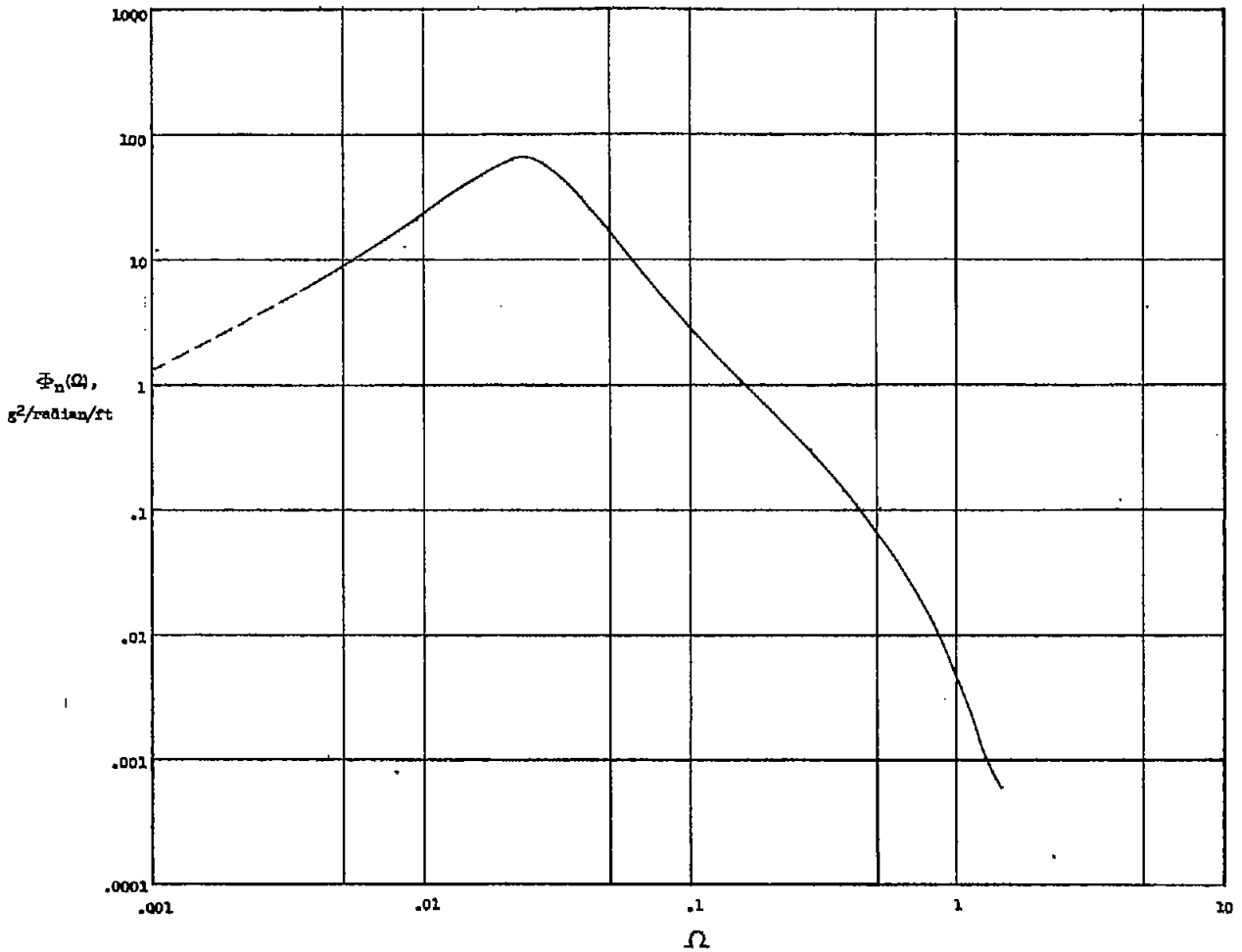

(c) $C_{h_{\delta_t}} = -175.$

Figure 6.- Continued.

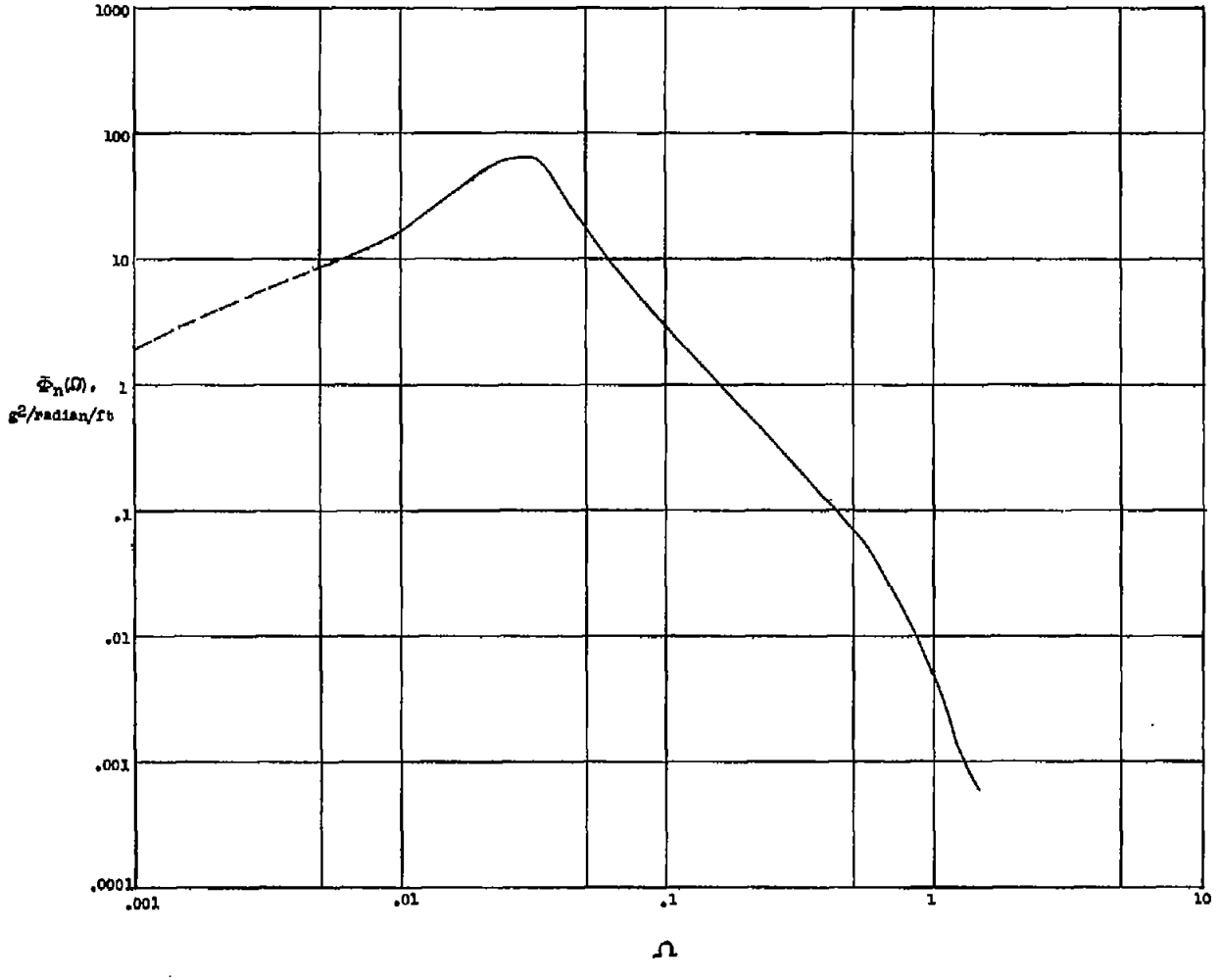

(d) C_{h_δ}, = -250.

Figure 6.- Continued.

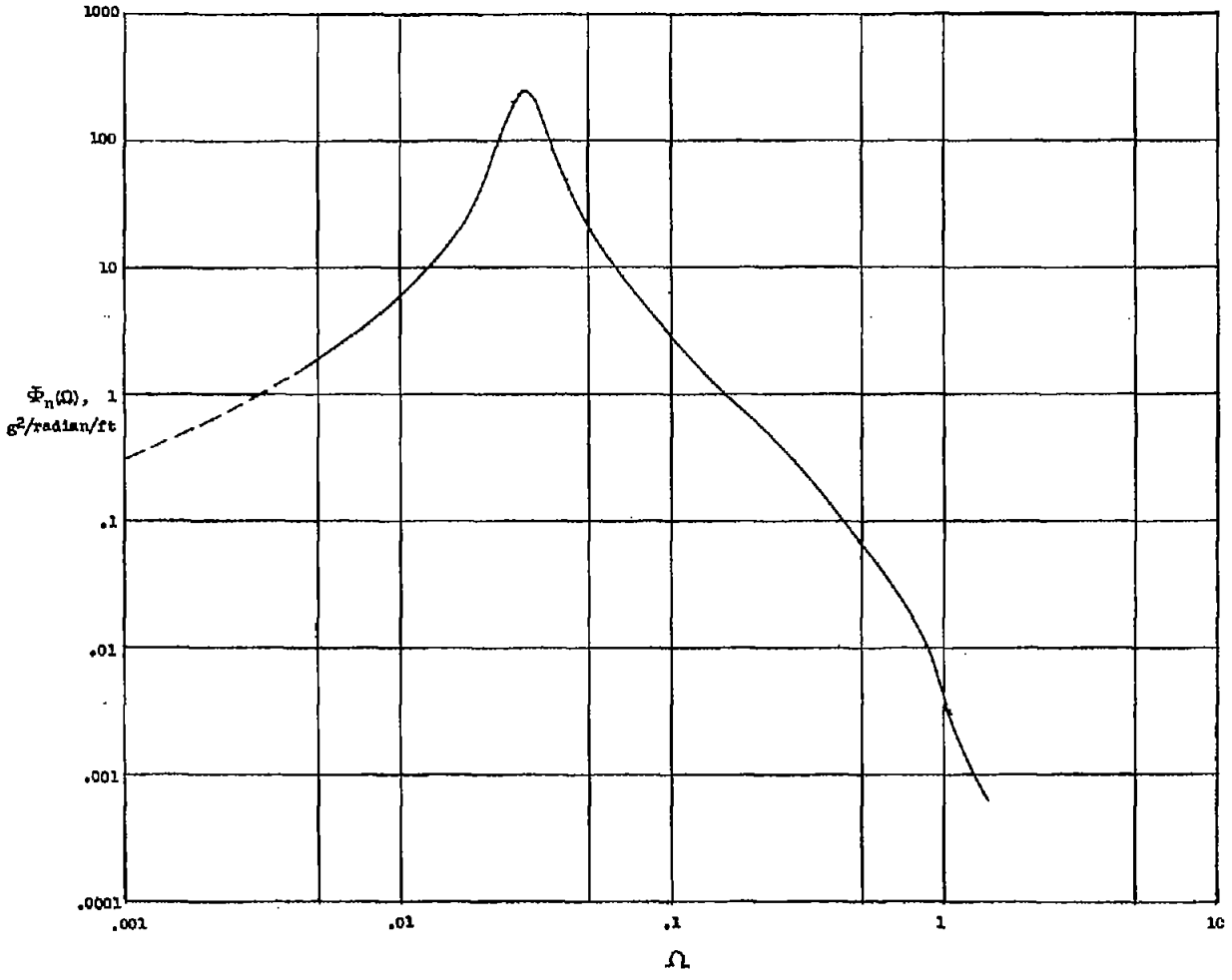

(e) $C_{h_{\delta'}} = -\infty$.

Figure 6.- Concluded.

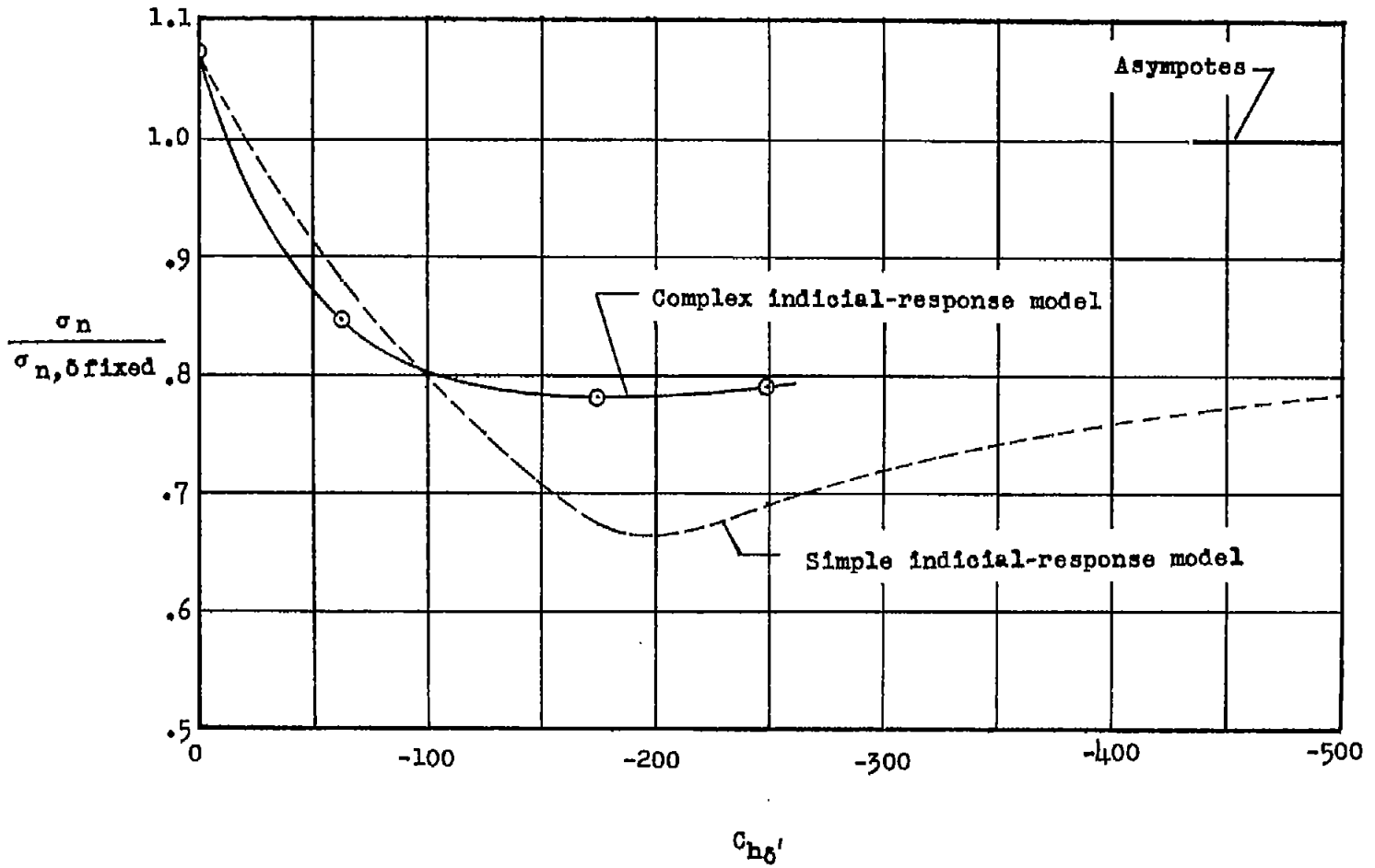

Figure 7.- Normalized root-mean-square value of normal-acceleration response as affected by variations in elevator viscous restraint.